НОВЫЕ ВОЗМОЖНОСТИ В ПРИМЕНЕНИИ РЕНТГЕНОВСКОЙ ПРЕЛОМЛЯЮЩЕЙ ОПТИКИ

Анатолий СНИГИРЕВ
ESRF, Grenoble, France

Фонд некоммерческих программ «Династия»

http://www.dynastyfdn.com/

Фонд Дмитрия Зимина
ДИНАСТИЯ

Проф. Владимир Бушуев

кафедра физики твердого тела физического факультета

Московского государственного университета им. М. В. Ломоносова

Foundation Dynasty

Prof. Vladimir Bushuev

Moscow State University, Moscow, Russia

SR Sources Worldwide

- New sources: Australia (Boomerang), Canada (CLS), China (???), France (SOLEIL), Germany (PETRA-III), Spain (ALBA), UK (DIAMOND),
- New projects: US (NSLS-II), Sweden (MAX-IV…
- The 3 large rings: APS (USA), ESRF (Europe), SPring-8 (Japan)

ESRF Members and Scientific Associates

Contribution to ESRF budget
(and share of beam time)

Members

• France	27.5%
• Germany	25.5%
• Italy	15%
• UK	14%
• Belgium/Netherlands	6%
• Spain	4%
• Switzerland	4%
• Denmark/Norway/ Sweden/Finland	4%
	<u>100%</u>

Scientific Associates

Current discussions with:

- <u>Russia</u>
- Slovakia
- Estonia, Latvia, Lithuania
- Ireland (?)
- Greece (?)

<u>MoU signed in Moscow at KCSR in 11 June 2008</u>

Russian scientists and ESRF strengthen cooperation

PRESS RELEASE - The Kurchatov Institute in Moscow (Russia) and the European Synchrotron Radiation Facility (ESRF) in Grenoble (France) have made a step towards a closer collaboration between the scientific communities of these two institutes. A Memorandum of Understanding was signed on 11 June 2008 in Moscow to promote the different areas of this collaboration.

13.06.2008

The Kurchatov Institute in Moscow.

The Memorandum foresees a joint research and development programme as well as exchange of scientists and scientific expertise with the aim of pushing forward common projects. In this framework, the two institutes will also organise joint workshops and conferences.

In his speech at the signing ceremony, the Head of the Russian Federal Agency for Science and Innovations, Prof. Sergey N. Mazurenko, emphasised the importance of scientific and technological links between the two laboratories. This statement was echoed by Prof. Michael V. Kovalchuk, the Director of the Kurchatov Institute.

In his reply, the Director General of the ESRF, Prof. William G. Stirling, expressed his admiration for the achievements of Russian scientists using synchrotron light and his desire to see a long-term relationship develop with the Kurchatov Institute and Russian scientists.

The Principal Elements of the Upgrade Programme

- Reconstruction of ~ 1/3 of the beamlines:
  Improved performance and routine nano-focus capabilities
- Extension of ~1/3 of the Experimental Hall:
  120 m long beamlines for nano-meter and nano-radian beams
- Upgrade of the accelerator complex:
  Very high brilliance and reliability of the X-ray source
- Development of new SR Instrumentation:
  To underpin the beamline and source improvements
- Enabling science-driven Partnerships:
  New science and applications

ESRF Council 22-25 November 2008

177 million Euros 2009-2015

List of beamlines

ESRF

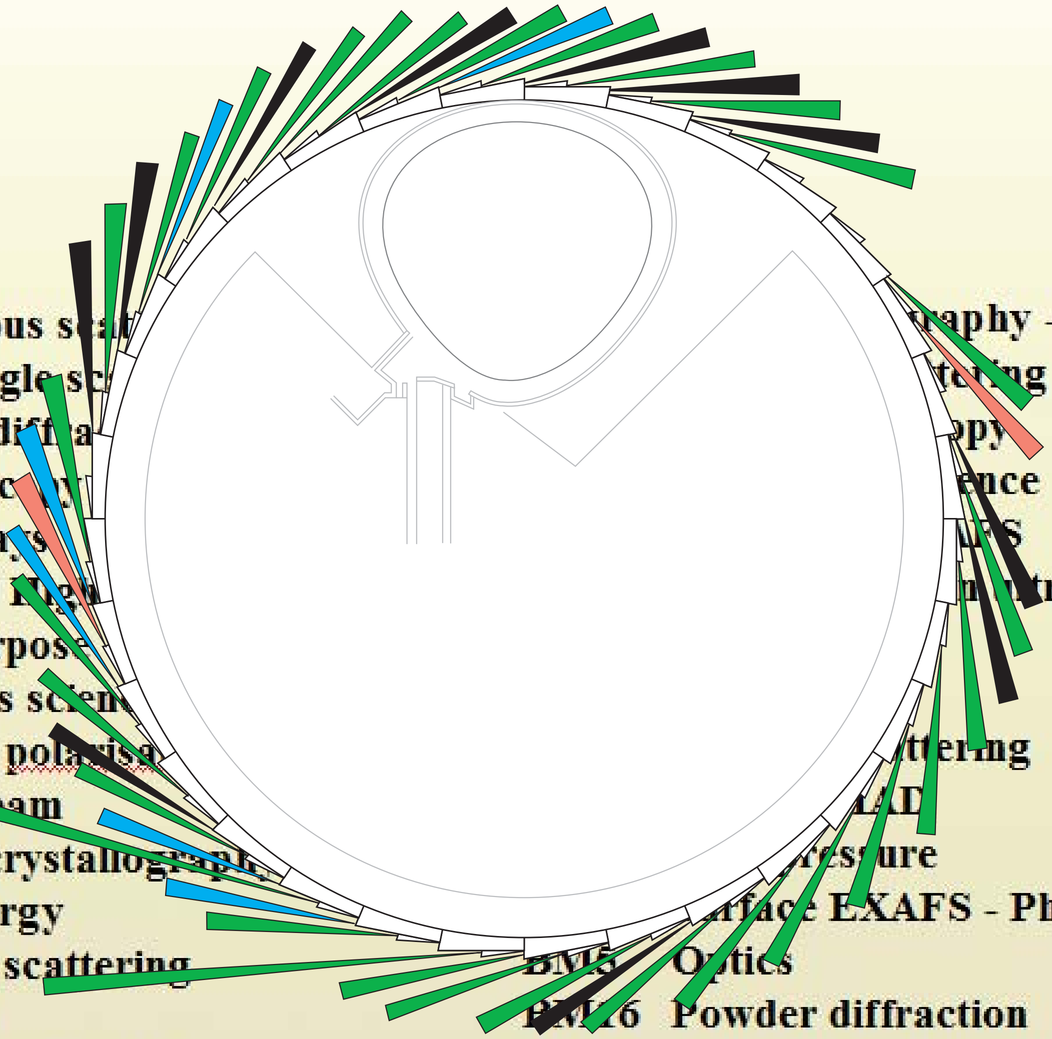

ID1 Anomalous scat
ID2 Small-angle sc
ID3 Surface diffra
ID8 Spectroscopy
soft X-rays
ID9 Biology / High
ID10 Multipurpose
ID11 Materials scien
ID12 Circular polarisa
ID13 Micro-beam
ID14 Protein crystallograph
ID15 High energy
ID16 Inelastic scattering
ID17 Medical
ID18 Nuclear scattering

raphy - Topography
tering
opy
ence
AFS
ultra-dilute
ttering
AD
ressure
rface EXAFS - Photoemission
BM5 Optics
BM16 Powder diffraction
BM29 Absorption spectroscopy

Buildings and BLs movements

Many BLs involved: estimation of the cost of several scenarios

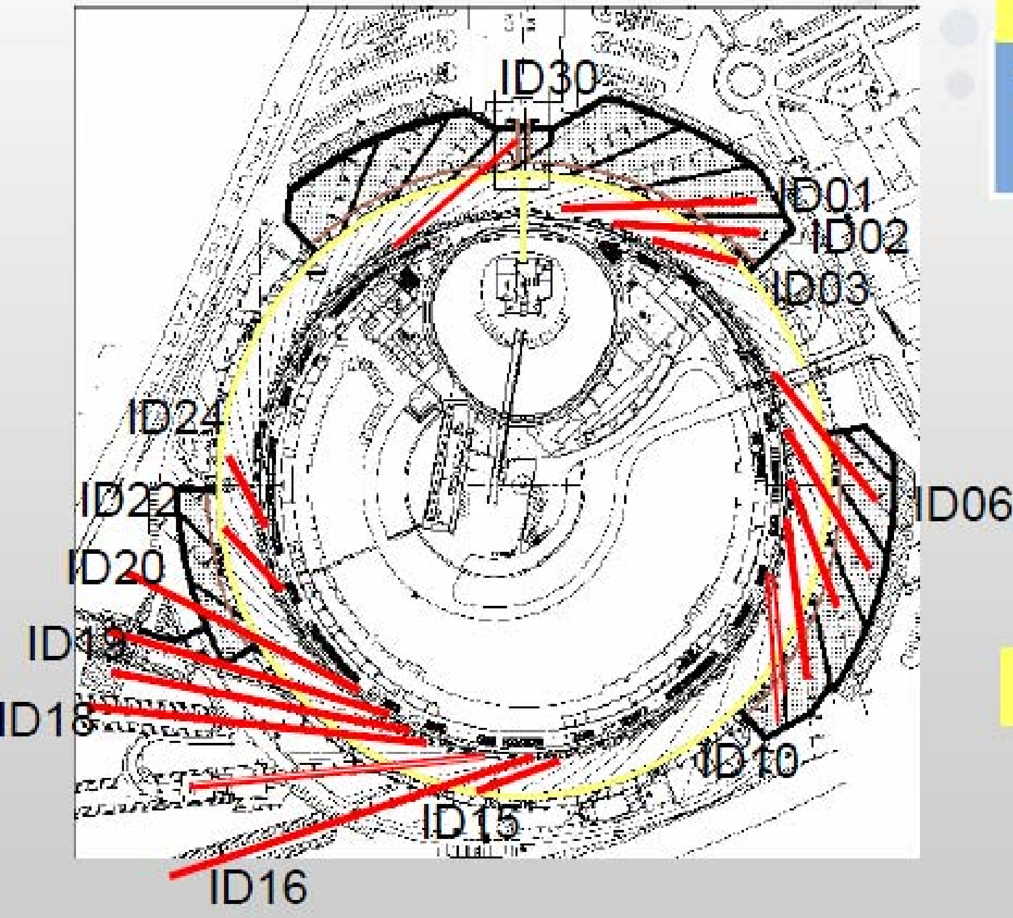

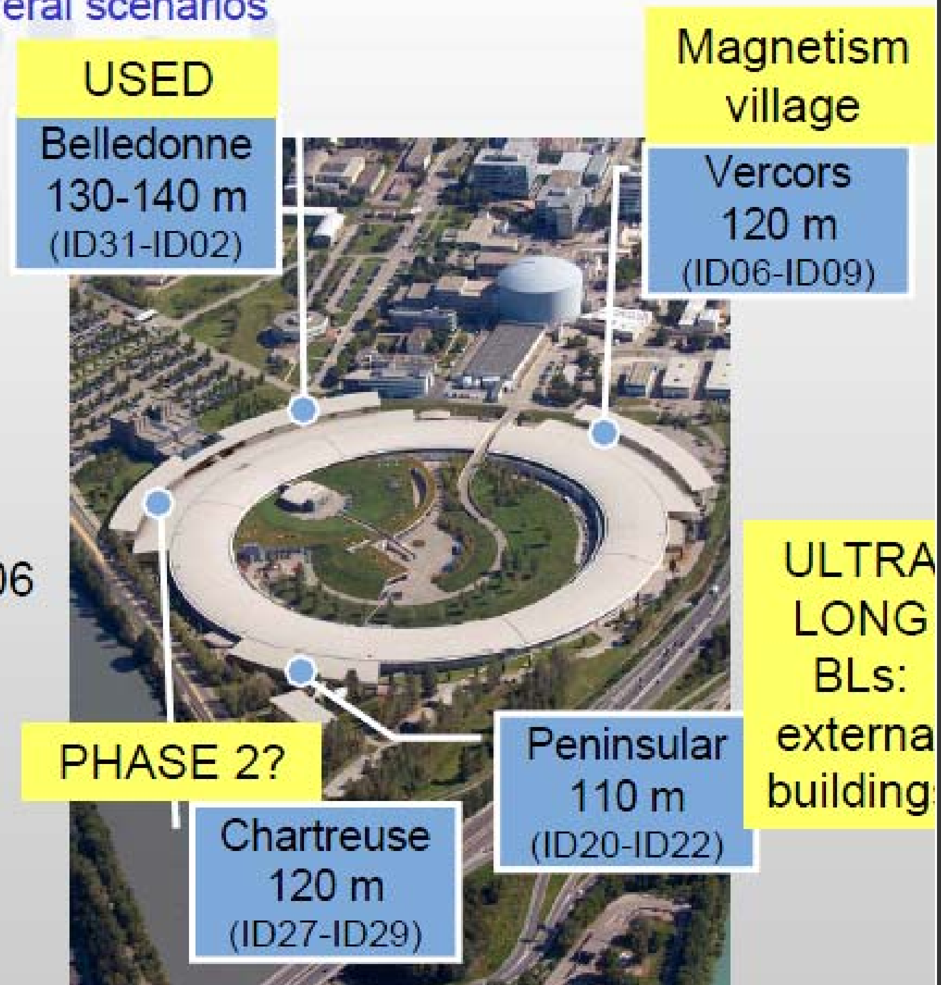

ESRF HIGHLIGHTS 2007

		Even ID (ID02, ID06...)	Odd ID (ID01, ID03...)	Even BM (BM02, 4,...) 3 mrad	Even BM (BM02, 4,...) 9 mrad	Odd BM (BM01, 3,...) 3 mrad	Odd BM (BM01, 3,...) 9 mrad
Magnetid Field	[T]	Variable	Variable	0.4	0.85	0.4	0.85
Horiz. beta functions	[m]	37.5	0.3	1.3	0.9	2.1	1.6
Horiz. dispersion	[m]	0.144	0.033	0.059	0.042	0.088	0.073
Horiz. rms e- beam size	[μm]	415	51	95	75	131	112
Horiz rms e- divergence	[μrad]	10.3	108	115	111	102	97.4
Vert. beta functions	[m]	3.0	3.0	41.2	41.7	31.6	31.7
Vert. rms e- beam size	[μm]	8.6	8.6	32	32	28	28
Vert. rms e- divergence	[μrad]	2.9	2.9	1.3	1.3	0.9	0.9

Table 2: Beta functions, dispersion, rms beam size and divergence for the various source points.

ESRF ID Source size (FWHM) :

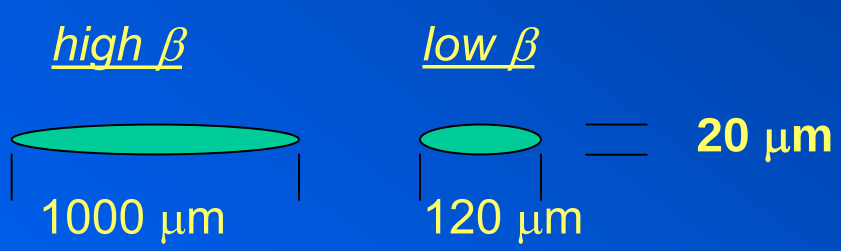

Undulator X-ray beam

ESRF 200 mA

10^{13} ph/s/mm^2/Si-111

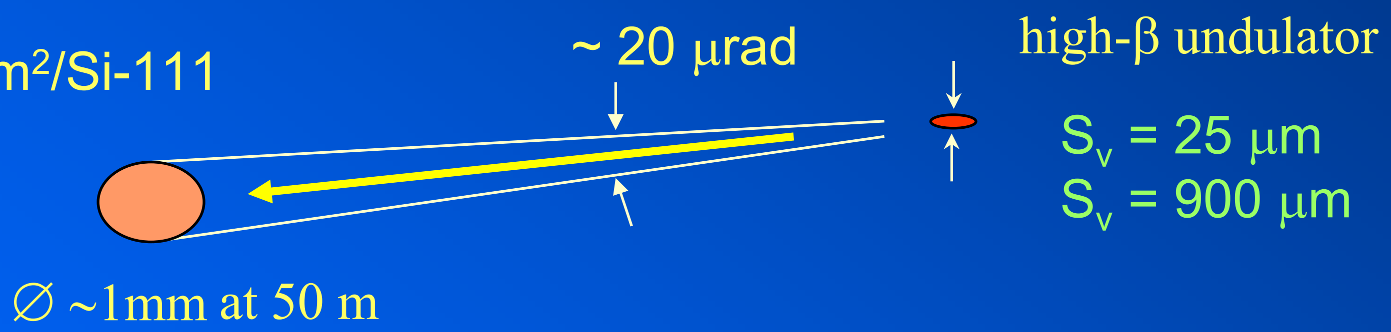

Temporal coherence $\lambda^2/\Delta\lambda$ – monochromaticity $\Delta\lambda/\lambda$

Si 111: 10^{-4}-10^{-5}

ML: 10^{-2}

- **Spatial coherence**

source size $S \sim 20\ \mu m$ spatial coherence $L\lambda/s$

source distance $L \sim 50\text{-}100$ m **$\sim 100\text{-}500\ \mu m$**

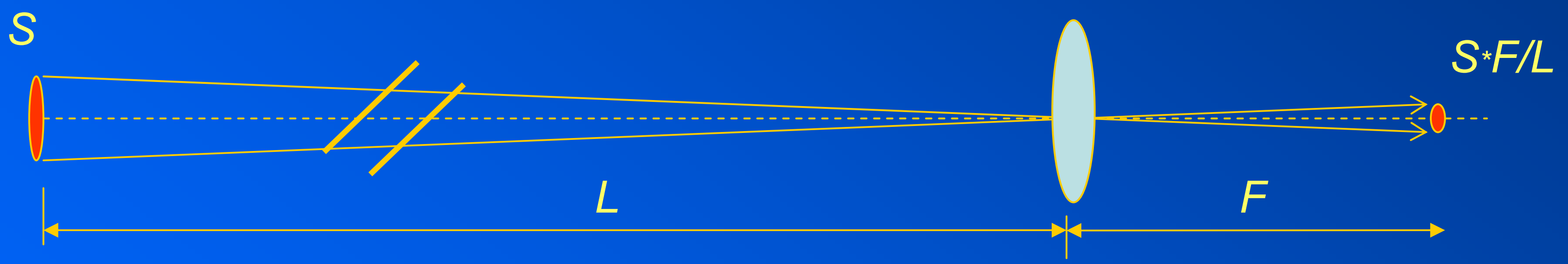

*For 100m BL: F=10 cm focus = S*F/L =* ***20 nm!***

angular source size: $< 0.4\ \mu rad$

Crystals: $\Delta d/d$ $< 10^{-6}$

Mirrors: slope error $< 10^{-6}$

Si-111 $\Delta\theta \sim 20\ \mu rad$ (λ =1Å, E = 12.4 keV)

Si-555 $\Delta\theta \sim 0.5\ \mu rad$ (λ =1Å, E = 30 keV)

Coherence Characterisation by Holography / Boron fiber

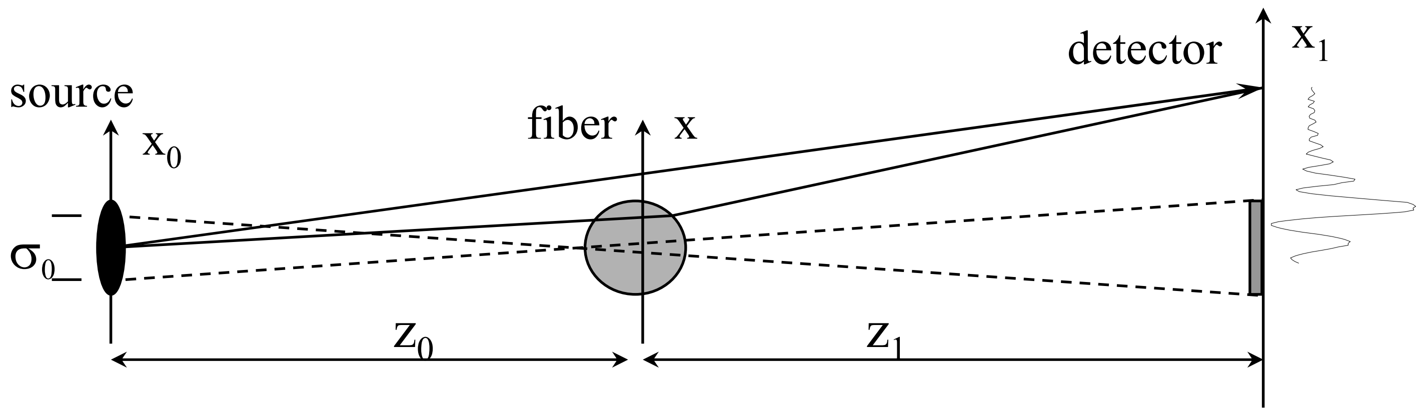

$$I(x_1) = 1 + A(x_1) + 2A(x_1)F(x_1)$$

$$A(x_1) = \frac{f_1 / 2(x_1)}{(1 + f(x_1))^{1/2}}, \quad f(x_1) = \frac{\alpha^2 R}{(x_1 - R)^3}, \quad \alpha = 2\delta z_1$$

$$F(x_1) = \cos\left(\pi \frac{(1-\beta^2)}{\lambda z1}(x_1 - R)^2\right) \exp\left(-\frac{(x_1 - R)^2}{\sigma_{mc}^2}\right),$$

$$\sigma_{mc} = \frac{2\lambda z_0}{\pi \sigma_0}$$

$$V(x_1) = \frac{I(x_1)_{\max} - I(x_1)_{\min}}{I(x_1)_{\max} + I(x_1)_{\min}}$$

$$\sigma_0 = \frac{z_0}{z_1}\frac{\lambda z_1}{(x_1 - R)} C(x_1), \quad C(x_1) = \frac{2}{\pi} \ln^{1/2}\left(\frac{V_0(x_1)}{V(x_1)}\right)$$

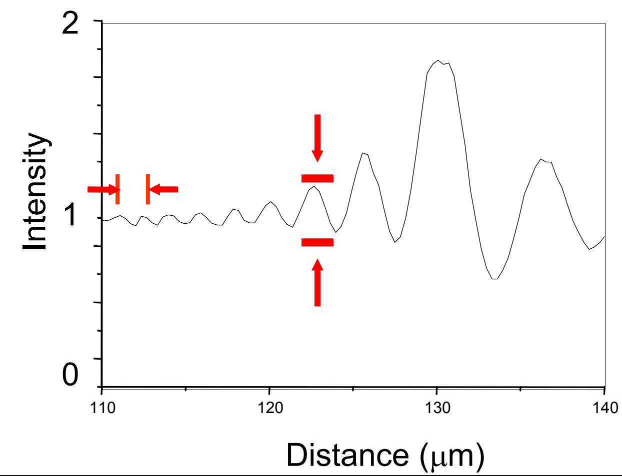

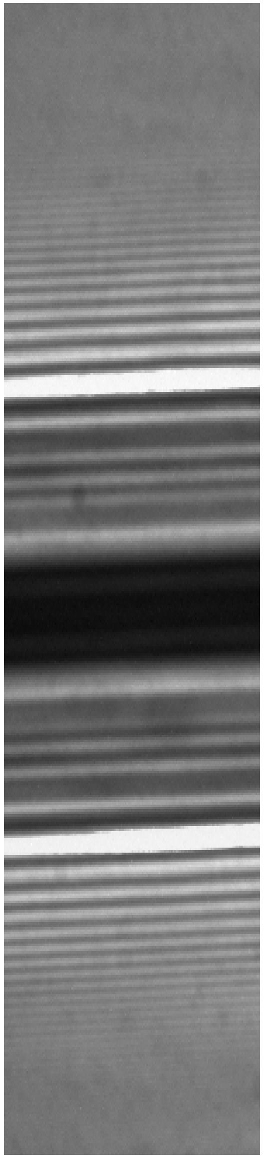

50µm

V. Kohn, I. Snigireva, A. Snigirev. Phys. Rev. Let. ***85****, 13, 2745 (2000)*

Techniques and Instrumentation Test Beamline
ID06 @ ESRF

Science and technology programme

- White beam development
- Microoptics test bench
- Detector test bench
- Large Volume Press
- Pulsed magnetic fields

Microoptics test bench at ID6

C. Detlefs, T. Roth

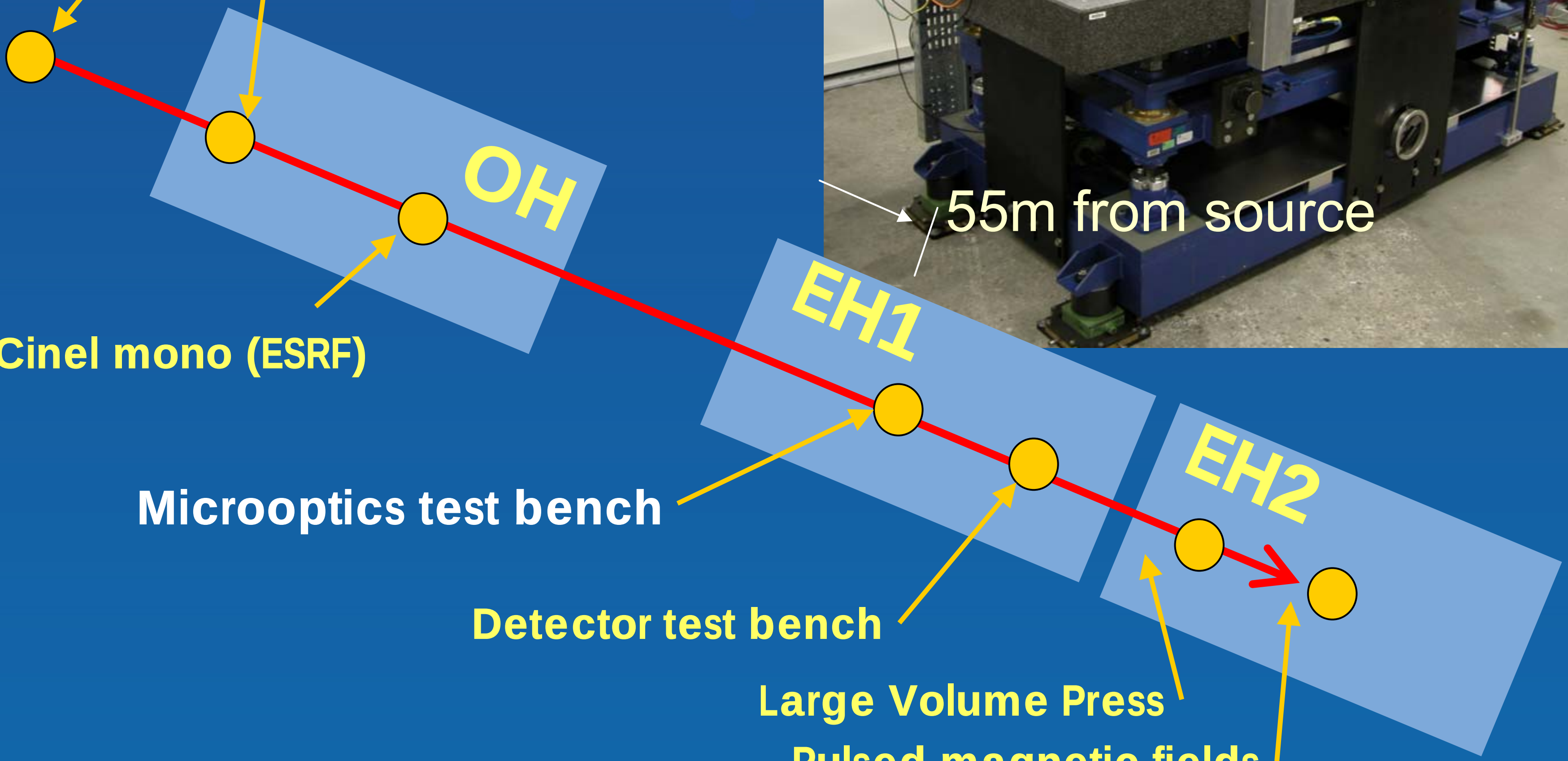

Focusing Optics for Hard X-rays (E > 6 keV)

	reflective				*diffractive*	*refractive*
	Kirkpatrick Baez systems		Capillaries	Waveguides	Fresnel Zone plates	Refractive lenses
	mirrors Kirkpatrick Baez, 1948	multilayers Underwood Barbee, 1986	Kreger 1948	Feng et al 1993	Baez 1952	Snigirev et al, 1996
	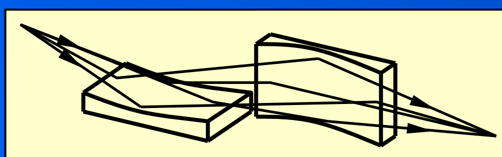		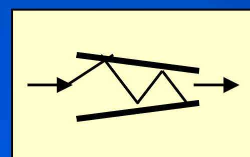	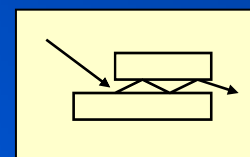	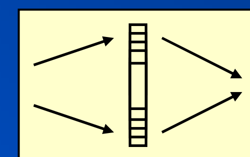	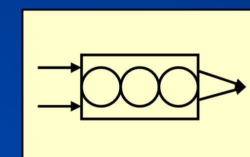
Energy	< 30 keV	< 80keV	< 20keV	< 20keV	< 30 keV (80)	<1 MeV
Bandwidth $\Delta E/E$	w. b.	10^{-2}	w.b.	10^{-3}	10^{-3}	10^{-3}
resolution	**25 nm** @15keV Mimura 2006	**41x45nm²** @24keV Hignette 2006	**50 nm** Bilderback 1994	**40x25 nm²** Salditt 2004	**30 nm** @20 keV Kang, 2006 **17 nm**, 2007	**50 nm@20keV** Schroer, 2004 **150nm@50keV** Snigirev,2006

Introduction to Capillary Optics

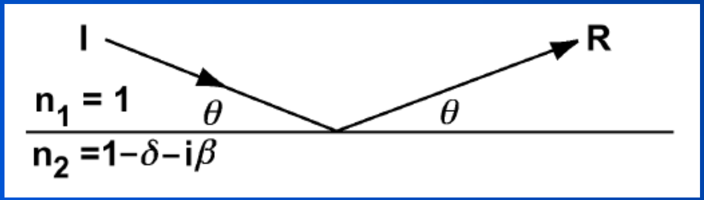

For Glass: θ_c (mrad) = 30 / E (keV)
2 mrad @ 15 keV
1 mrad @ 30 keV

Multi-Bounce Glass Capillary

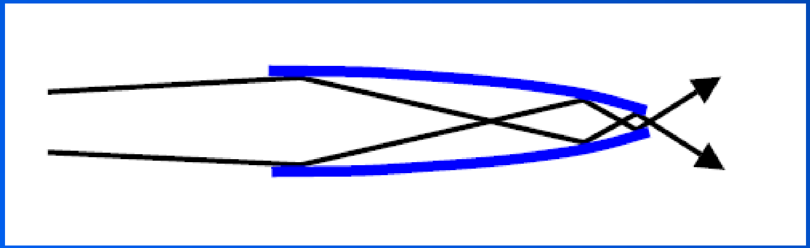

Easy!
to make small focal spot < 1 μm

50 nm!
D. H. Bilderback, S. A. Hoffman, D. J. Thiel
*Science, 1994, **263**, 201.*

Short working distance (sub-mm scale)
Low transmission

One-Bounce Glass Capillary

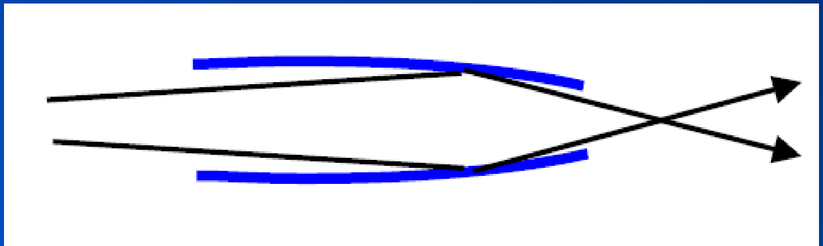

Large working distance (cm scale)
Near 100% transmission

Challenge!
to make small focal spot < 1 μm

Short and compact –
may fit in spot that is too short
for KB mirror assembly!

First really useful elliptical x-ray optic
-Balaic, Nugent, Barnea, Garrett, Wilkins,
J. Synch. Rad. 1995; 2: 296.

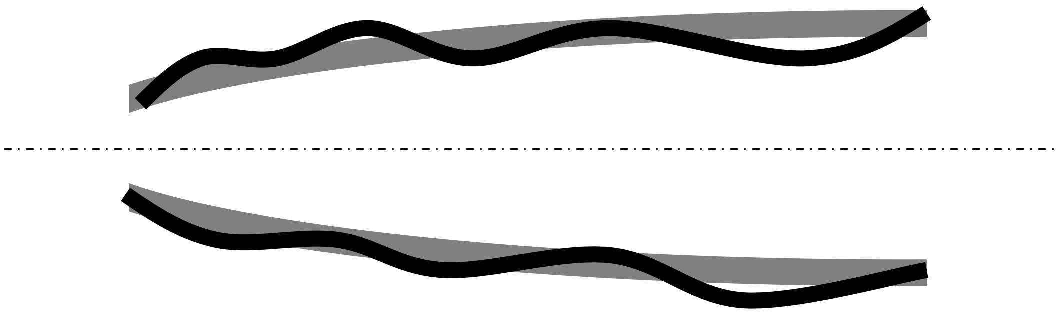

average slope errors:

- centreline straightness
  (circular symmetry)
- figure errors

resolution

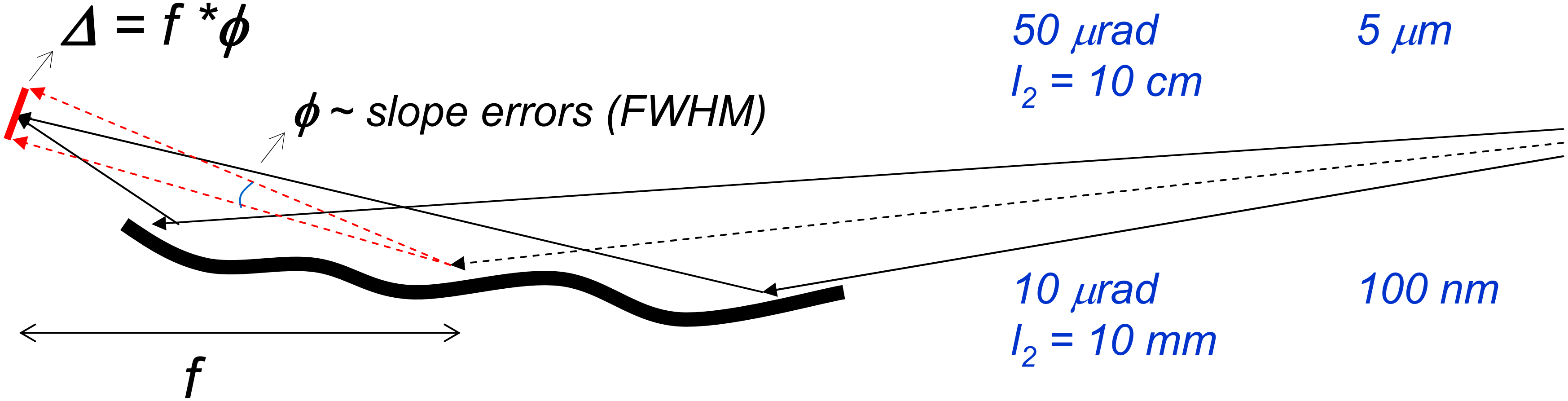

50 μrad | *5 μm*
l_2 = *10 cm*

10 μrad | *100 nm*
l_2 = *10 mm*

2 step focusing using single-bounce ellipsoidal capillary combined with Fresnel zone plate.

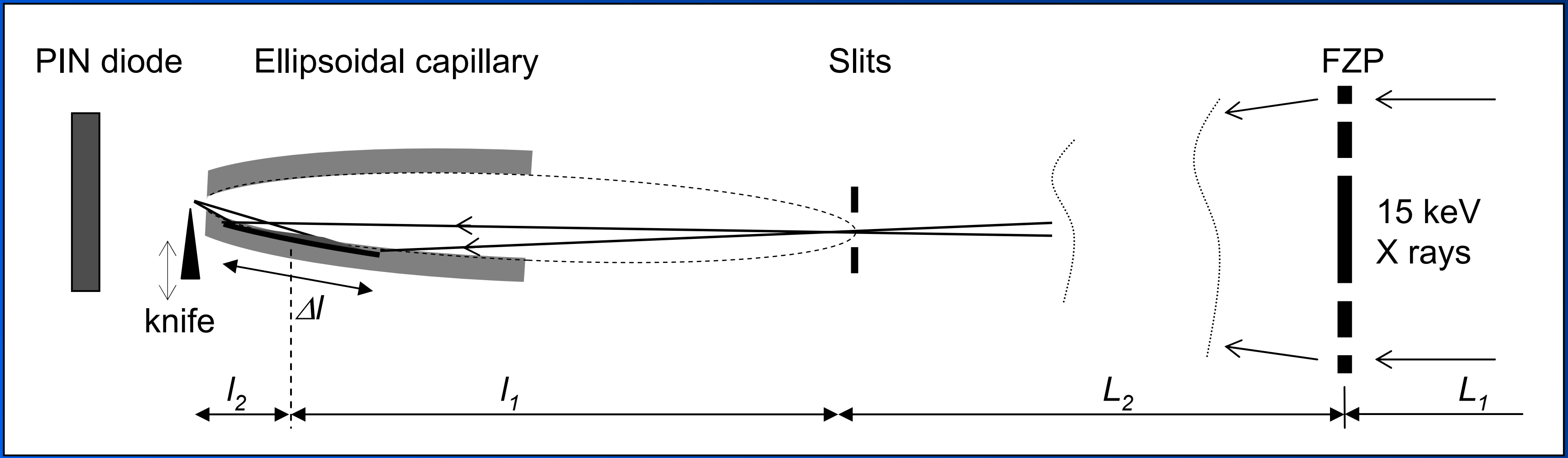

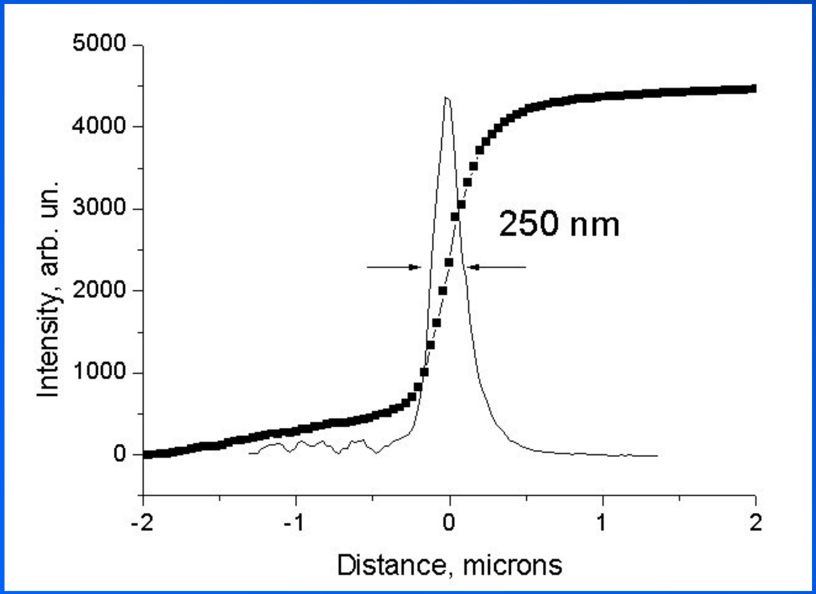

l_1 = 27.5 mm
l_2 = 2.5 mm

α = 0.08 mrad
M = 11
Δl = 5 mm

<u>0.25 μm !!!</u>

Fresnel Zone Plate (FZP)

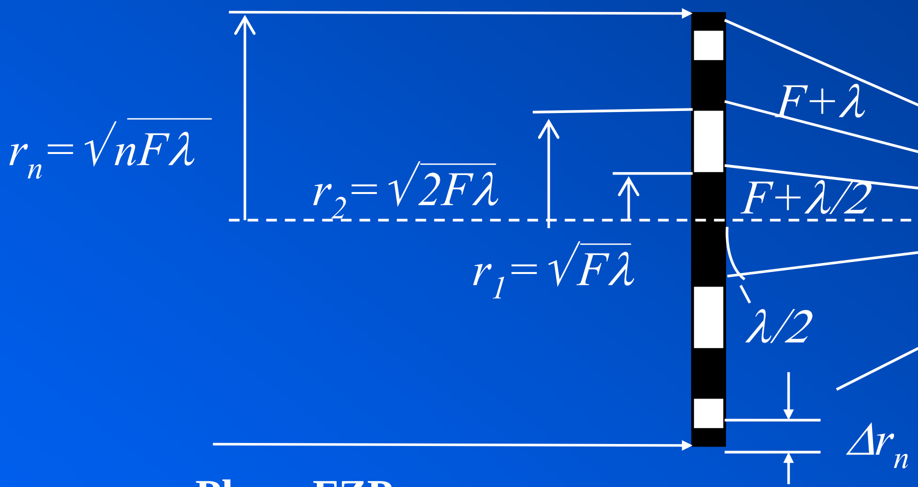

FZP parameters

A = 100 - 1000 µm
Δr_n = 0.05 - 0.3 µm
t_{Si} = 1 - 10 µm
F = 60 cm at at 4 - 12 keV
flux 10^{10} photons/sec

Phase FZP
alternate zones -
phase shifting
efficiency ~ 40%

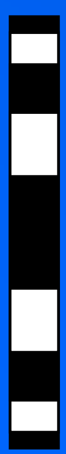

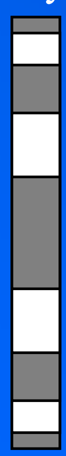

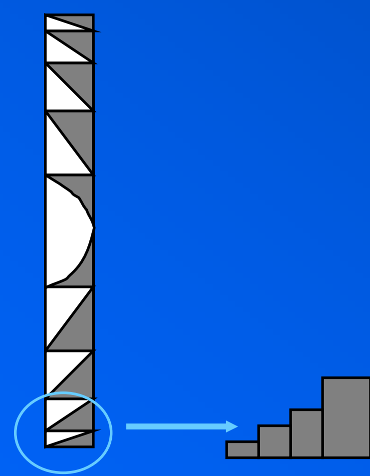

Amplitude FZP
alternate zones - opaque
efficiency ~ 10%

Kinoform FZP
(sawtooth profile)
efficiency ~ 70 - 100%

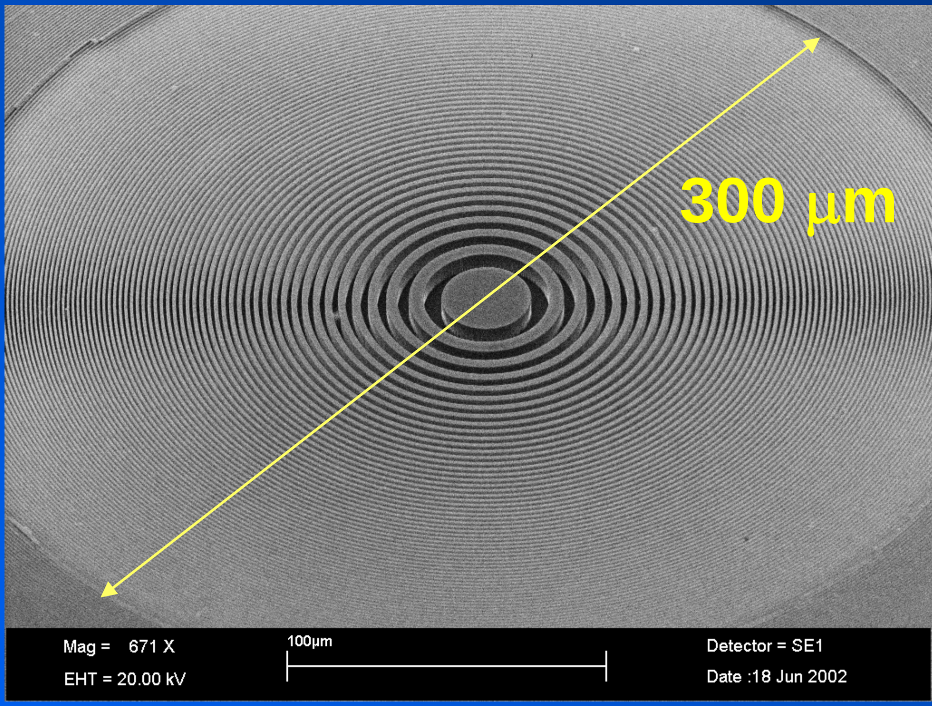

Res. ~ from 500 nm to 50 nm

FZP for hard X-rays (E > 5 keV)

APS: Au FZP (collabor. With Wisconsin)
outermost zone width ~ 0.1 μm
X-Radia: 30-50 nm 20-50 k$
ML Laue FZPs

Spring-8: Ta FZP (NTT AT)
outermost zone width ~ 0.1- 0.2 μm
Y. Kagoshima - 50 nm FZP at 10 keV
jelly-rolled FZP (N. Kamijo) – imaging at 80 keV

ESRF: Au, Ni etc. (collabor. PSI, Swiss and ELLETRA, Italy)
outermost zone width ~ 0.1- 0.2 μm
Si FZPs outermost zone width ~0.4 μm

SEM images

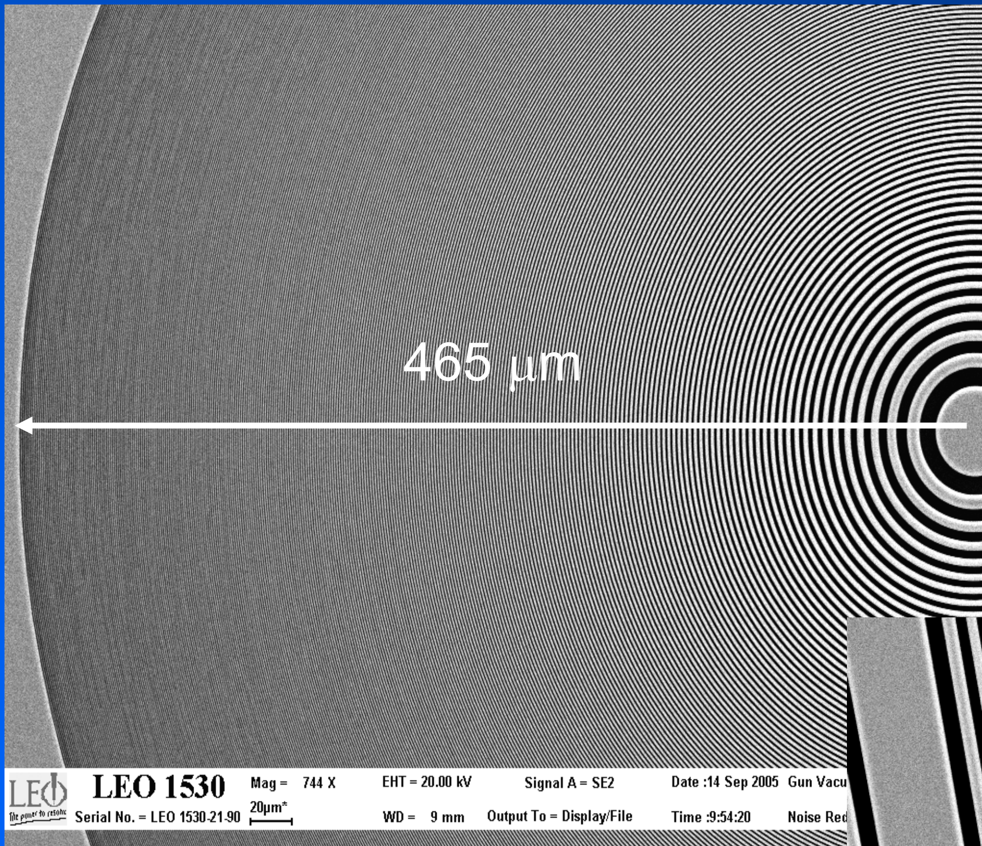
465 µm
LEO 1530
Mag = 744 X
EHT = 20.00 kV
Signal A = SE2
Date :14 Sep 2005
Serial No. = LEO 1530-21-90
20µm*
WD = 9 mm
Output To = Display/File
Time :9:54:20

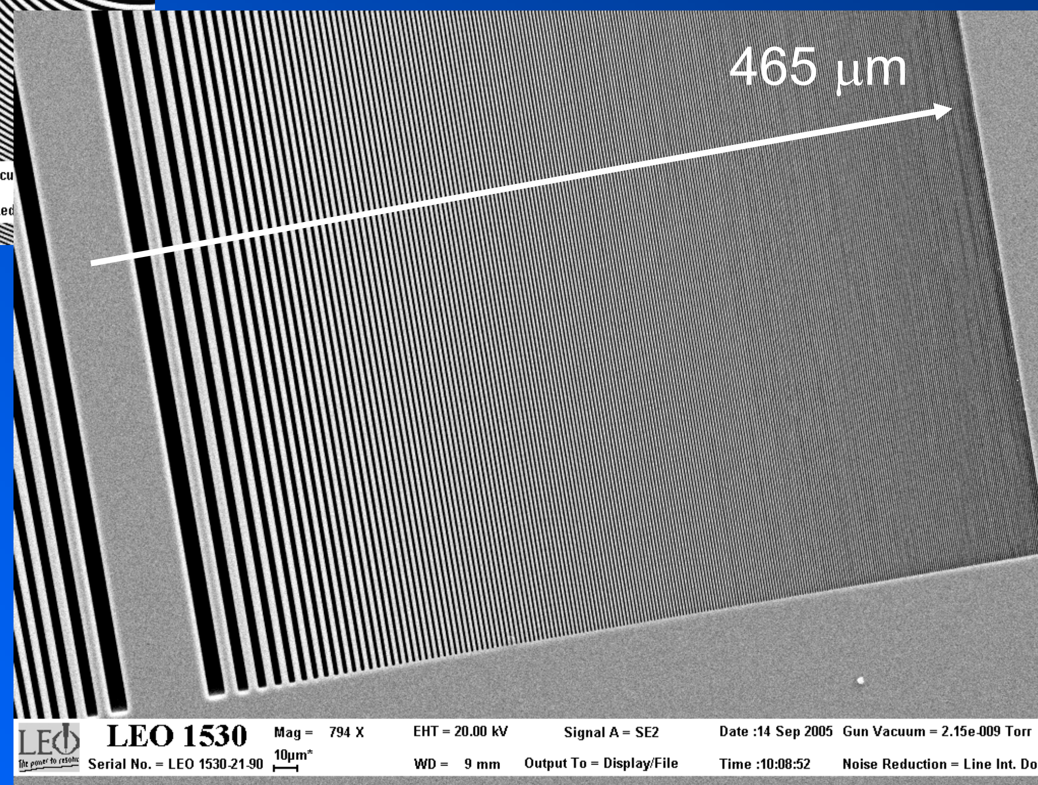
465 µm
LEO 1530
Mag = 794 X
EHT = 20.00 kV
Signal A = SE2
Date :14 Sep 2005
Gun Vacuum = 2.15e-009 Torr
Serial No. = LEO 1530-21-90
10µm*
WD = 9 mm
Output To = Display/File
Time :10:08:52
Noise Reduction = Line Int. Done

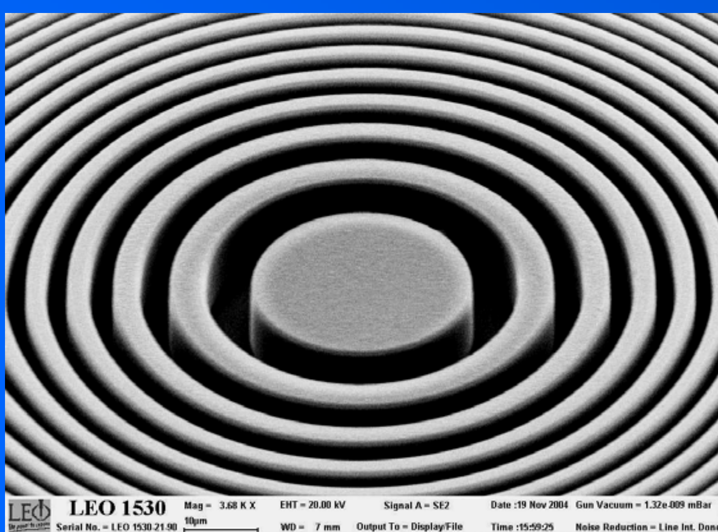
LEO 1530
Mag = 3.68 K X
EHT = 20.00 kV
Signal A = SE2
Date :19 Nov 2004
Gun Vacuum = 1.32e-009 mBar
Serial No. = LEO 1530-21-90
10µm
WD = 7 mm
Output To = Display/File
Time :15:59:25
Noise Reduction = Line Int. Done

FZP Si chip

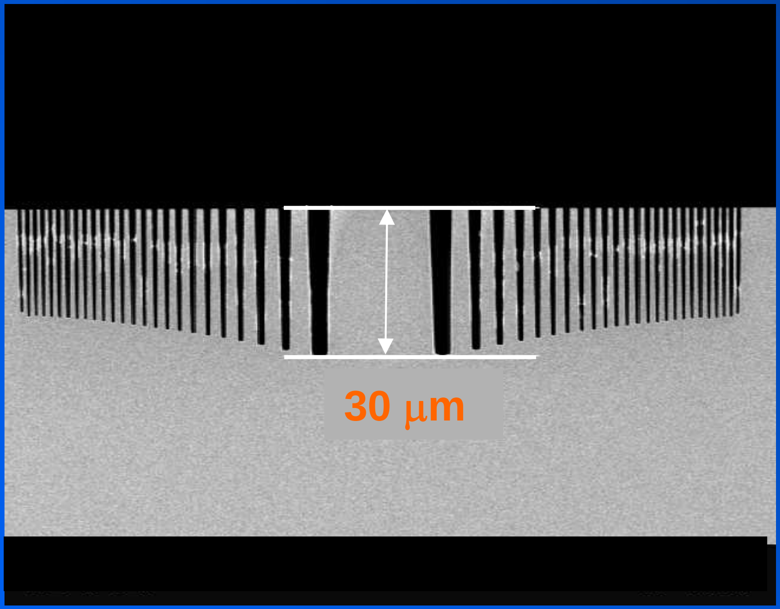

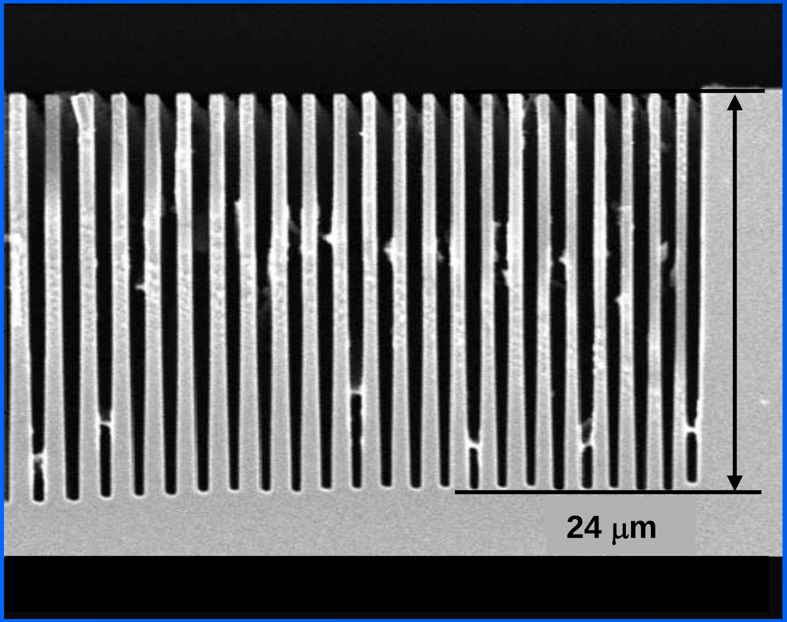

Chip	T_m / h, μm	E_{range}, keV	η_{max}, %	E_{max}, keV
DOE-4	12 / 9	6 - 12	30	7.5
DOE-5	80 / 16	11 - 21	26	14
DOE-7	90 / 30	17 - 40	32	23

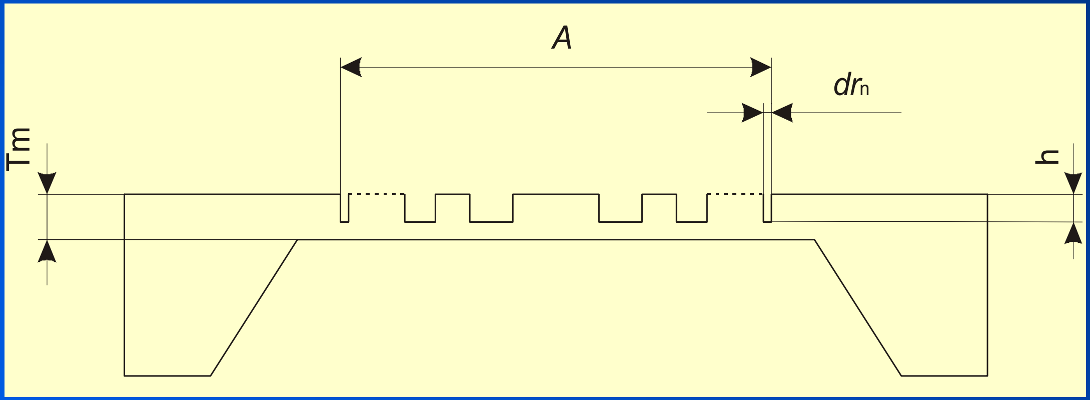

T_m, μm	thickness of Si membrane
h, μm	maximum height of zones
E_{range}, keV	energy range where focusing efficiency >**20**%
η_{max}, %	maximum focusing efficiency
E_{max}, keV	energy at which η_{max} maximum is achieved

aspect ratio ~50 !!!

X-ray Compound Refractive Lenses

$$F = \frac{R}{2\,\delta}$$

Re(n)= *1*-δ +*i*β < 1

$1\text{-}n \sim 10^{-5}\text{-}10^{-6}$

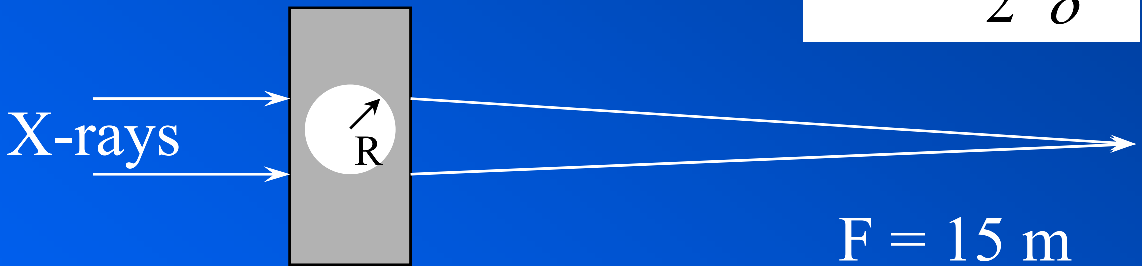

F = 15 m

A. Snigirev, V. Kohn,
I. Snigireva, B. Lengeler
Nature, Vol. 384, 49, 1996

Be
E = 10 keV
$\delta = 3.4*10^{-6}$
R = 100 µm

x N

$$F = \frac{R}{2\,N\,\delta}$$

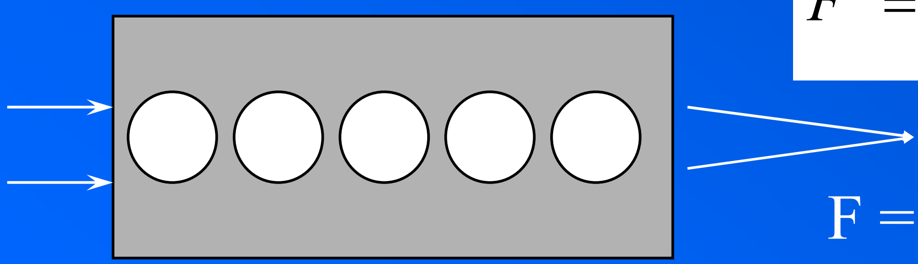

F = 0.5 m

N = 30

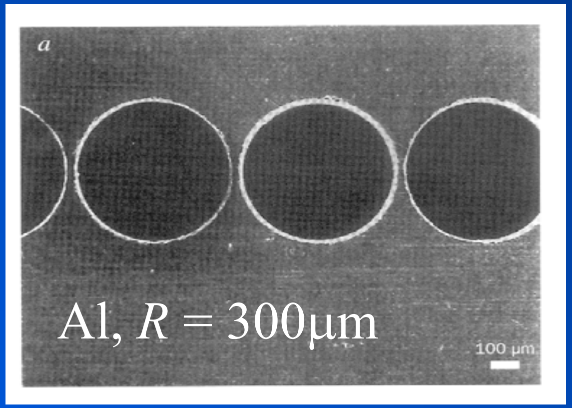

LETTERS TO NATURE

NATURE · VOL 384 · 7 NOVEMBER 1996

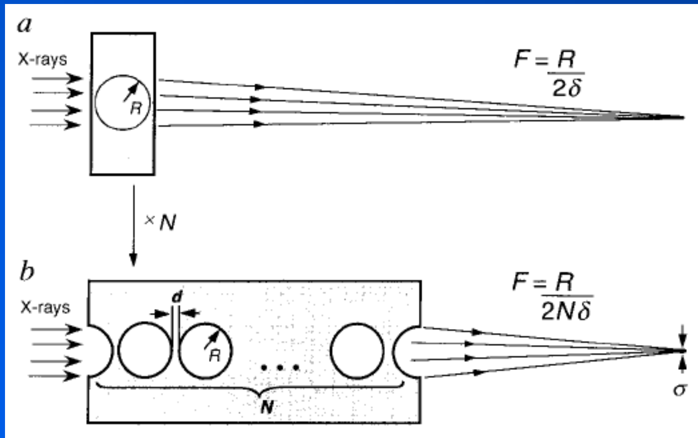

A compound refractive lens for focusing high-energy X-rays

A. Snigirev*, V. Kohn†, I. Snigireva* & B. Lengeler*‡

* European Synchrotron Radiation Facility, BP220, F-38043 Grenoble Cedex, France
† Kurchatov, I. V., Institute of Atomic Energy, 123182 Moscow, Russia

The first AL CRL

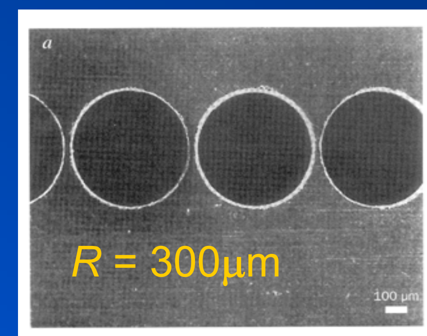

Si parabolic lens

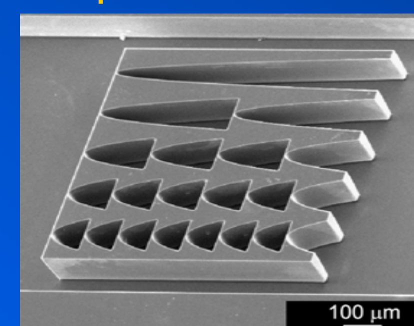

Refractive optics after 10 years development

standard tool at SR beamlines worldwide.
~ 50% of ESRF beamlines use refractive lenses

the most versatile and adaptable X-ray optics

- energy range -from a few keV to hundreds of keV
- focal length -from a few millimeters to tens of meters
- focal spot -from tens of nanometers to tens of microns
- microradian collimation
- high stability and low cost

applications: microdiffraction, microfluorescence and imaging, standing wave microscopy *etc.*

Russian collaborators: **Kurchatov Institute,** Moscow
IMT RAS, Chernogolovka

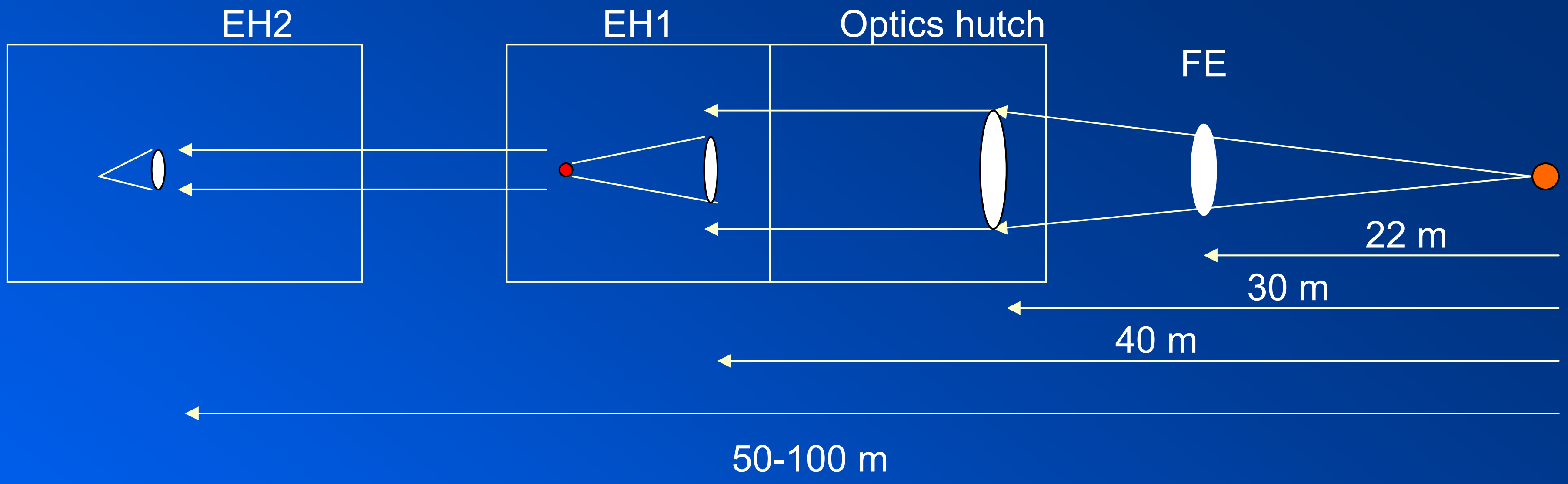

Refractive optics:

Condensers/collimators	**F ~ 10 m**	**10 μm**
Micro-optics	**F ~ 1 m**	**1 μm**
Nano-optics	**F ~ 10-100 mm**	**10 – 100 nm**

Energy range:

CRL 10 – 100 – (1000) keV

Reftractive optics / Materials

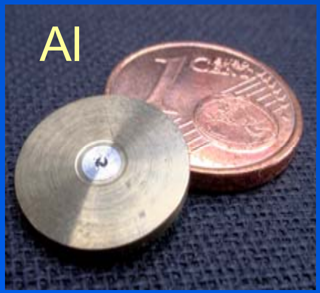

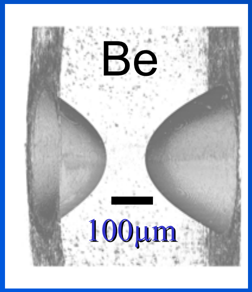

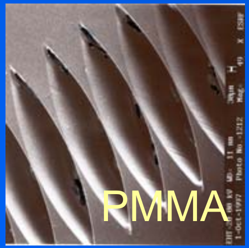

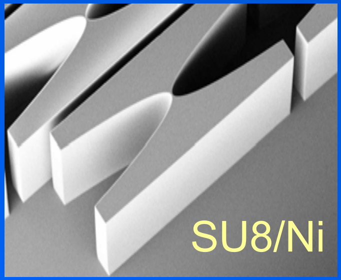

material	mode	E, keV	F, m	resolution, µm
Al	microfocus	18	0.3	0.48
	Imaging/tomo	25	1	0.3/0.4
Be	microfocus	12	0.5	1
	imaging	12	0.5	0.11
PMMA	microfocus	12	1	10
SU8	microfocus	14	0.2	0.27
Ni	microfocus	40-120	0.5	0.8
diamond	microfocus	9	0.5	2.2
glassy carbon	microfocus	25	0.03	1.4
Si planar	microfocus	14	0.25	0.6
Si nanolens	microfocus	15	0.03	0.05

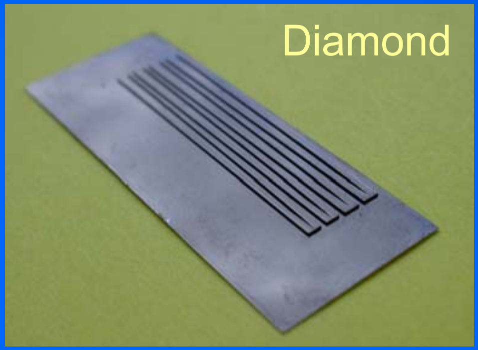

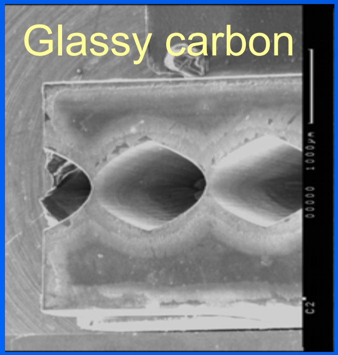

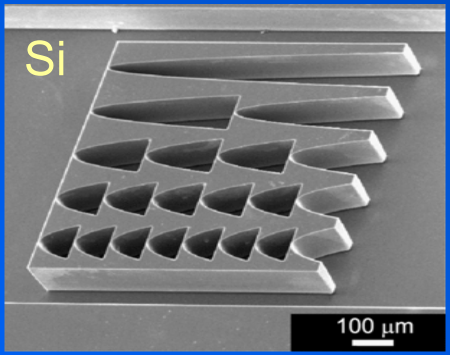

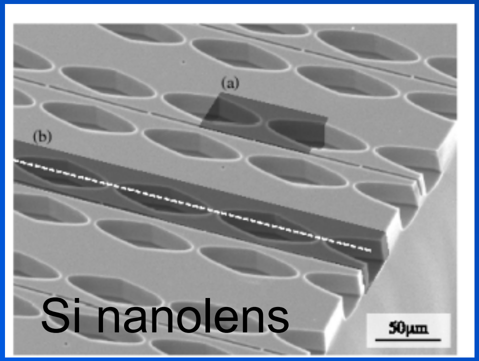

Parabolic Compound Refractive Lenses

Collab. B.Lengeler, C.Schroer,
RWTH, Aachen, Germany

single lens

$$F = \frac{R}{2N\delta}$$

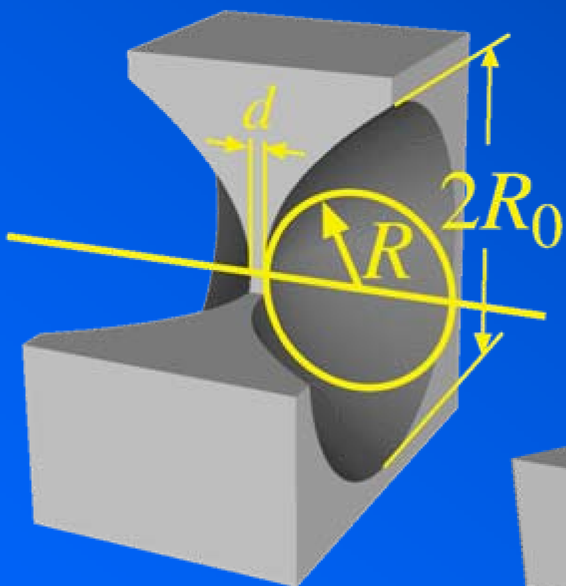

stack of lenses:
compound refractive lens (CRL)

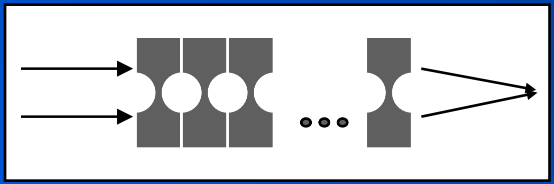

Al, Be

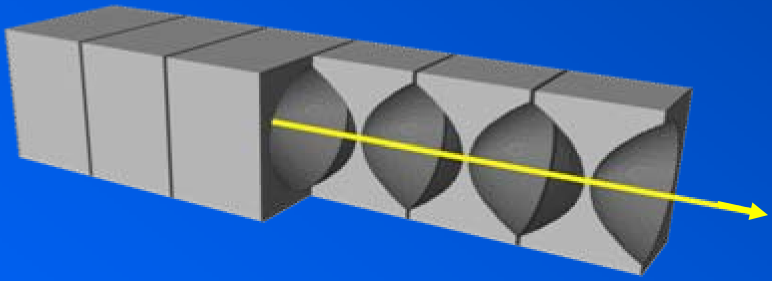

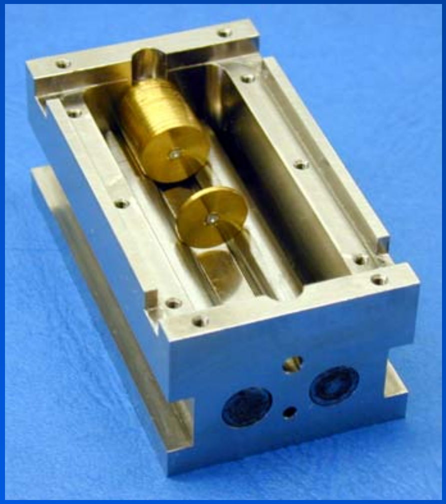

$R = 0.2\text{mm}$
$2R_0 = 0.9\text{mm}$
$d \approx 5\mu\text{m}$

R = 0.5mm
$2R_0$ = 2-3 mm

variable number of lenses: $N = 10 \ldots 300$

CRL transfocator   Energy range 10 -100 keV

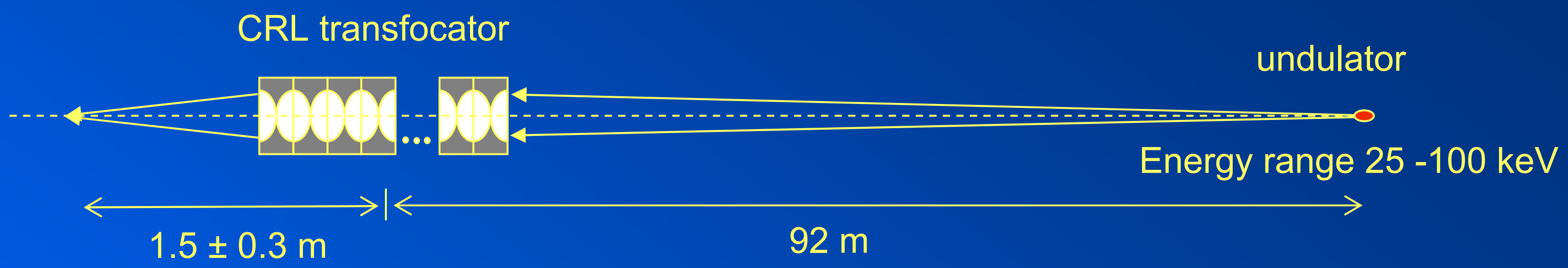

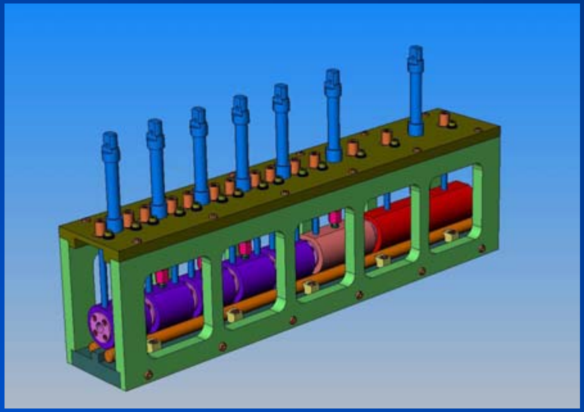

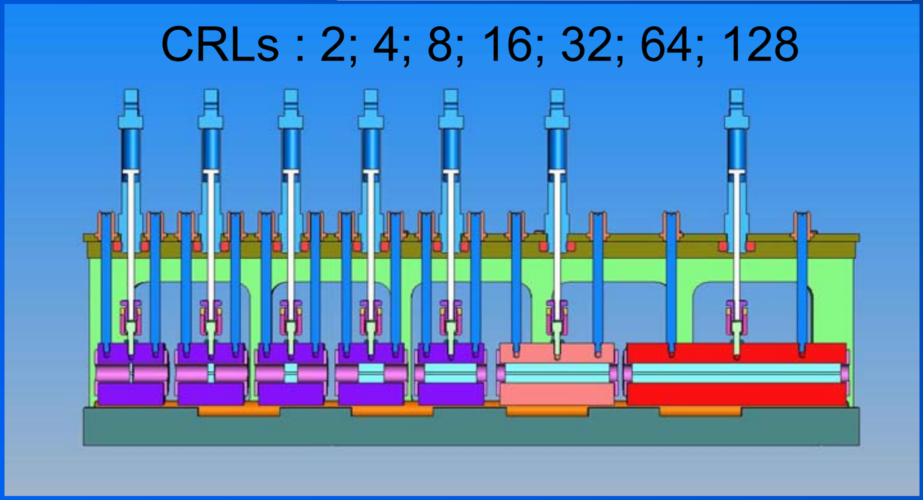

Cinel X-ray Refractive Lens Transfocator

(in-vacuum/white beam) ID11

cartridge and lenses

lens and cartridges assembly	5.12.08
chamber assembly	8.12.08
installation at ID11	January 2009
test / commissioning	Jan-Feb 2009

actuators

32 + 64 = 96 Al lenses
1 + 2 + 4 + 8 + 16 + 32 = 63 Be lenses

cartridges
with Be lenses

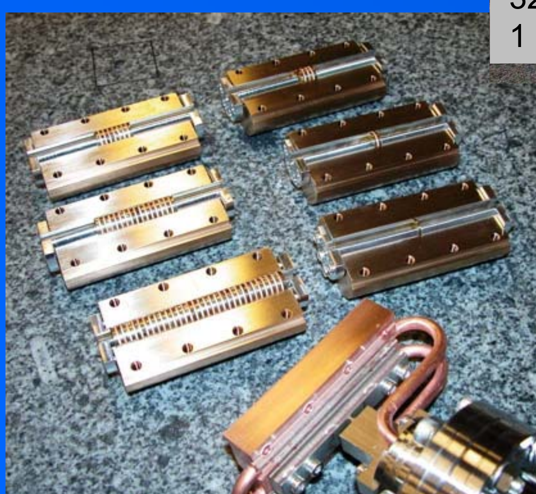

vacuum chamber

aboard view

Fourier Transform Diffraction/Imaging

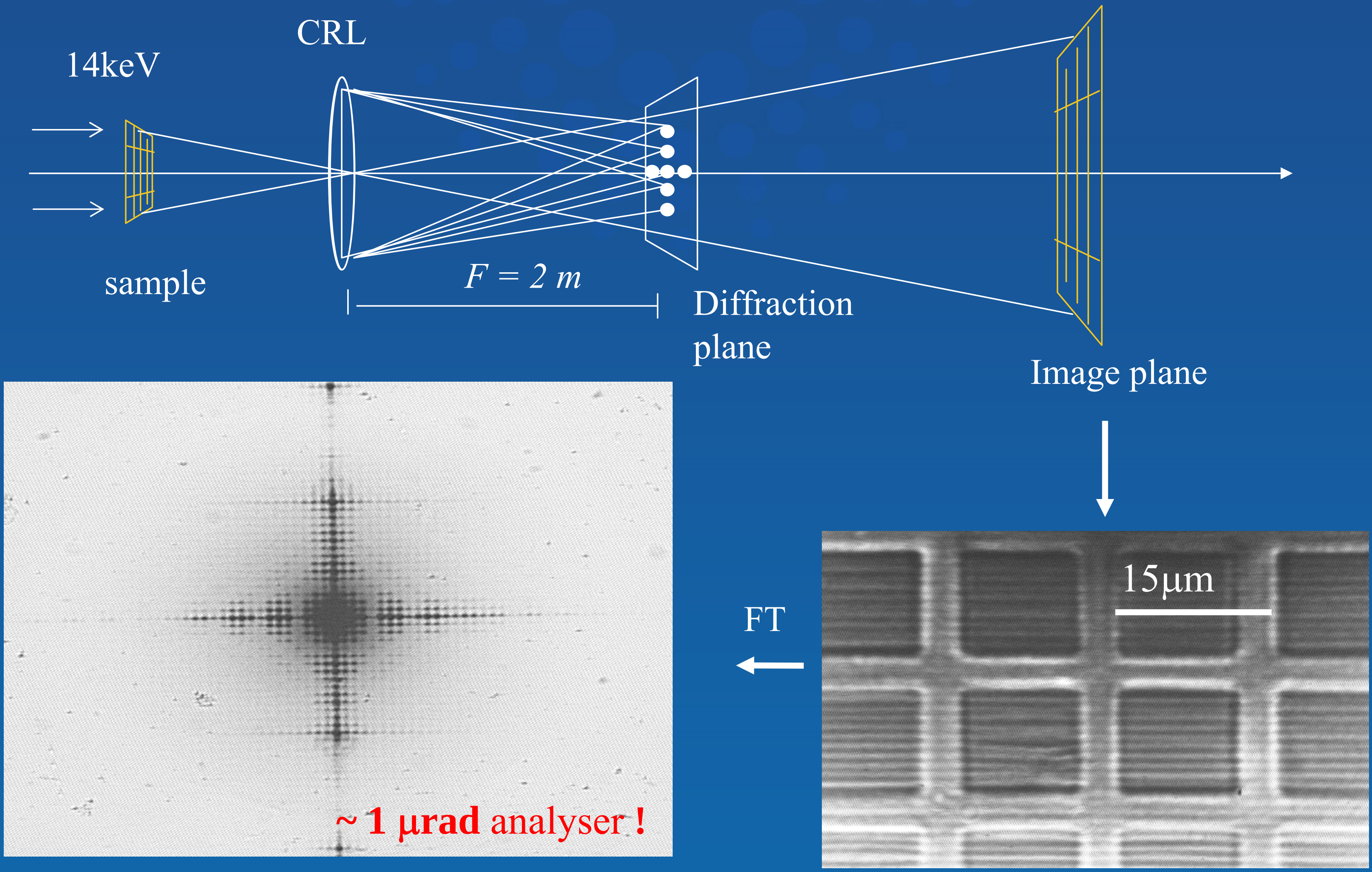

X-ray High Resolution Diffraction Using Refractive Lenses

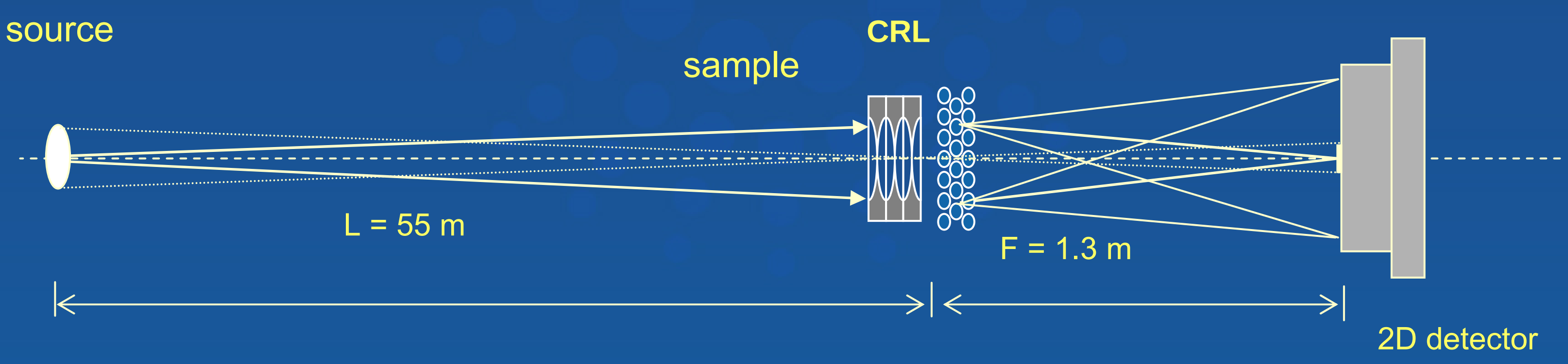

E = 28 keV
Al CRL, N = 112
F = 1.3 m

HR CCD det 2 μm resolution

resolution is limited
by angular source size:
s/L ~ 1 μrad

Si photonic crystal pitch - 4 μm

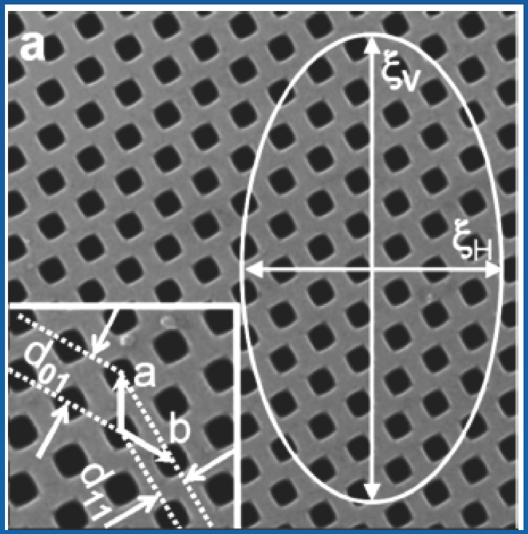

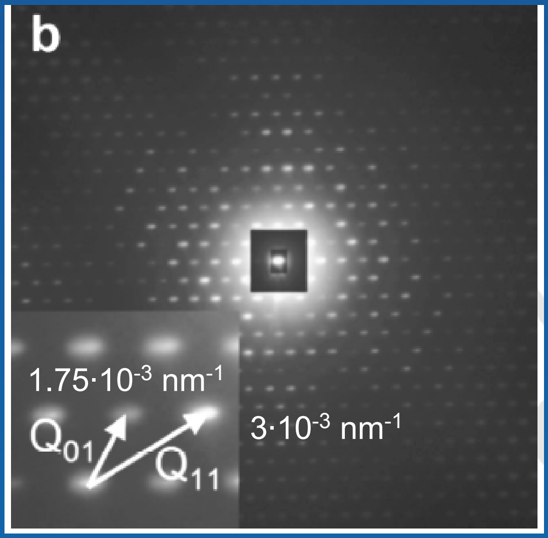

M. Drakopoulos, A. Snigirev, I. Snigireva, J. Schilling, Applied Physics Letters, 86, 014102, 2005.

Microradian x-ray diffraction

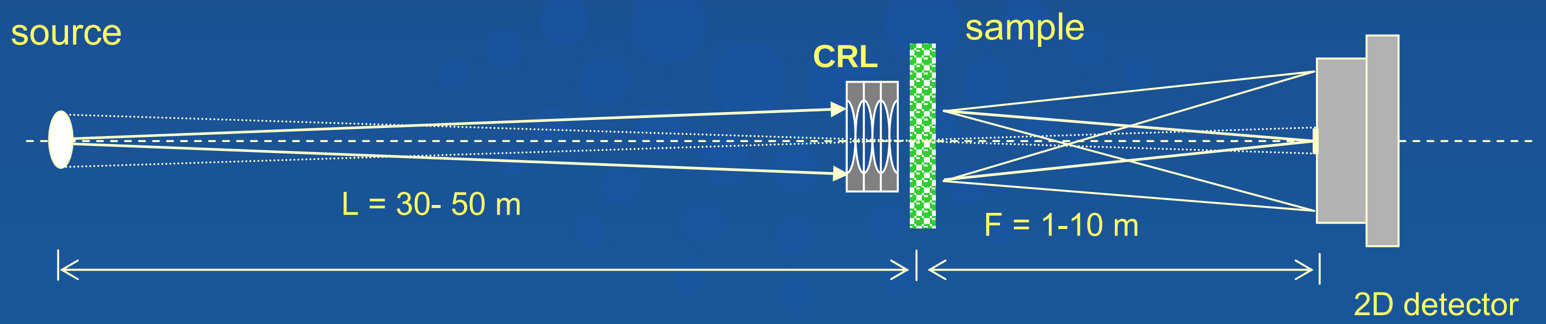

A versatile tool to study novel functional materials with nano- to micro-scale structure.

It allows

- 3D structure determination on the scale of 10s nm – 10s microns
- probing positional order on distances up to 100 microns
- quantitative characterization of various types of disorder (stacking disorder, domain size, microstrain, etc)
- to identify the superstructure built by pores in the membrane
- to measure the width of the Bragg peaks, thus quantitatively probing the long-range order.
- to study the spatial distribution of the crystalline grains along the substrate surface by taking measurements at different lateral positions in the samples and to construct the domain maps.

Diffraction patterns of colloids made from polystyrene spheres (425 nm)

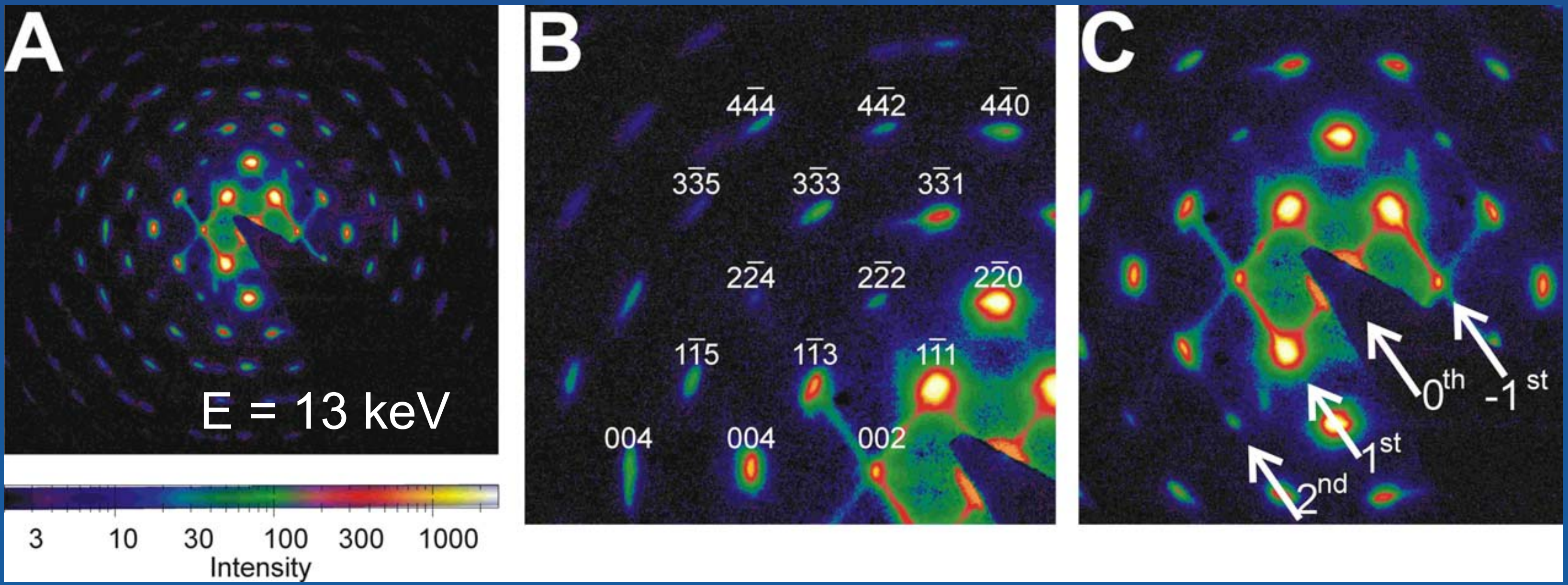

Clear face-centred cubic structure

- **Presence of sliding defects**
- **These defects are crucial in generating …ABCABC… stacking order**

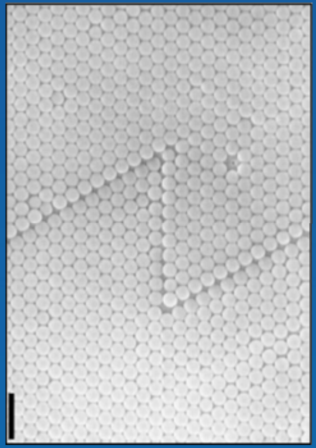

Panel A displays a full diffraction pattern while a zoom into one quarter is given in B along with the crystallographic assignment of the peaks. Again, the relative weakness of the 002, 222 and 224 reflections can be understood on the basis of Fig. 1C. A closer look on the central part of the pattern reveals presence of the Bragg rods, which are caused by the presence of the stacking disorder.

Spotlight on science

Stacking faults in colloidal photonic crystals revealed by microradian X-ray diffraction

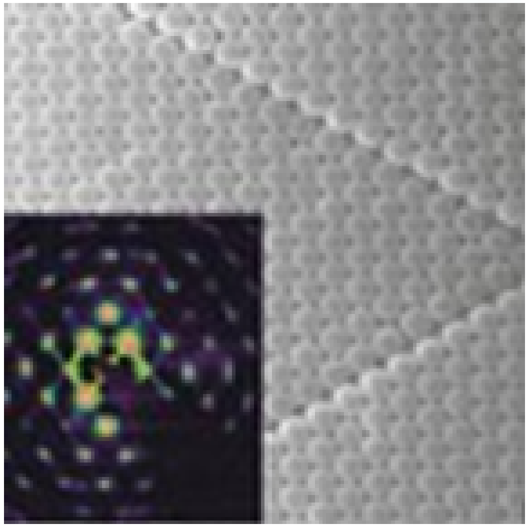

24-11-2009

The presence of a network of intersecting stacking faults in self-assembled colloidal crystals was demonstrated with X-ray diffraction with microradian resolution. These defects can seriously affect the optical properties of photonic materials fabric ... **Read More...**

Lens chip design

F = 10cm @ E = 10 - 50 keV

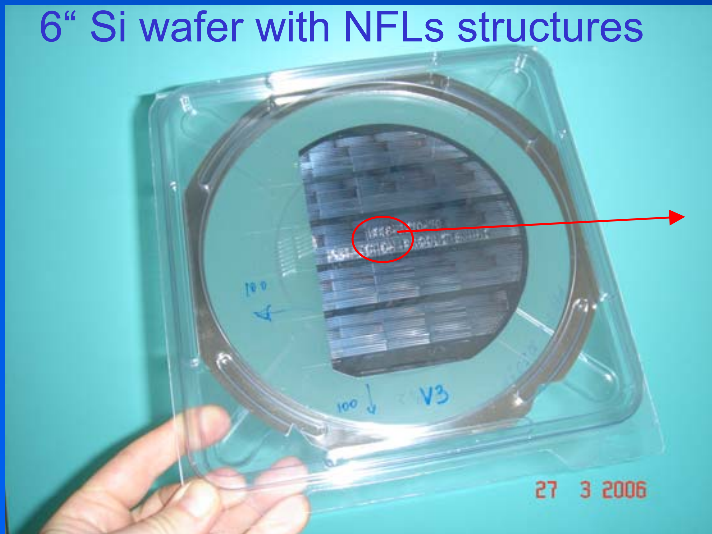

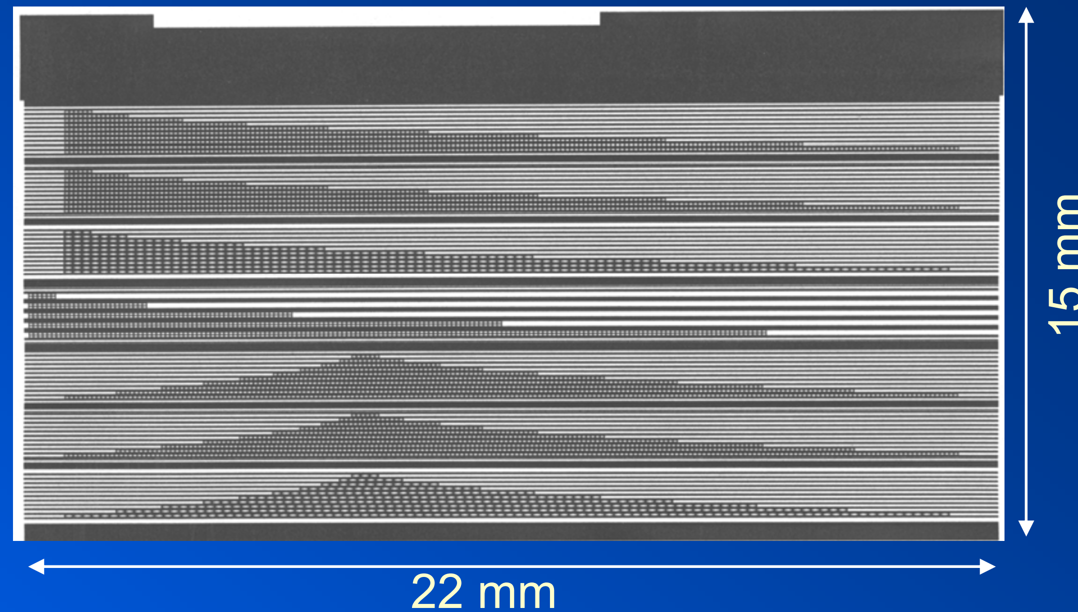

NN	Energy (keV)	Single lens length (µm)	Number of lenses	Radius of parabola apex (µm)	Total lens length (µm)
1	10	50 100	12 6	6.25 3.13	620 614
2	15	50 100	28 14	6.25 3.13	1436 1422
3	20	50 100	52 26	6.25 3.13	2660 2634
4	25	50 100	80 40	6.25 3.13	4088 4048
5	30	50 100	116 58	6.25 3.13	5924 5866
6	35	50 100	160 80	6.25 3.13	8168 8088
7	40	50 100	208 104	6.25 3.13	10616 10512
8	45	50 100	264 132	6.25 3.13	13472 13340
9	50	50 100	324 162	6.25 3.13	16532 16370
10	55	50 100	392 196	6.25 3.13	20000 19804

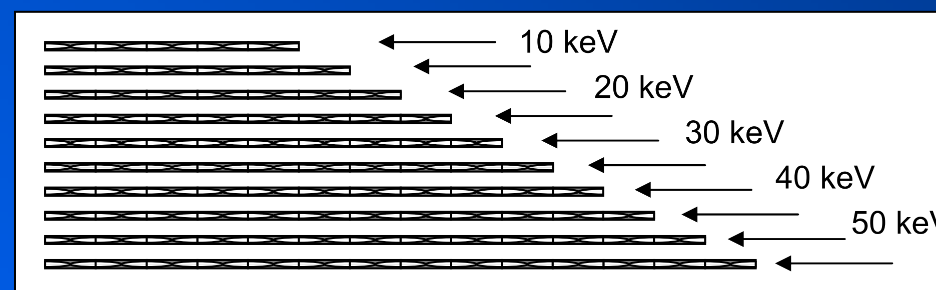

10 lenses per set

7 sets

~ 70 CRLs !

Схема изготовления Si преломляющих линз

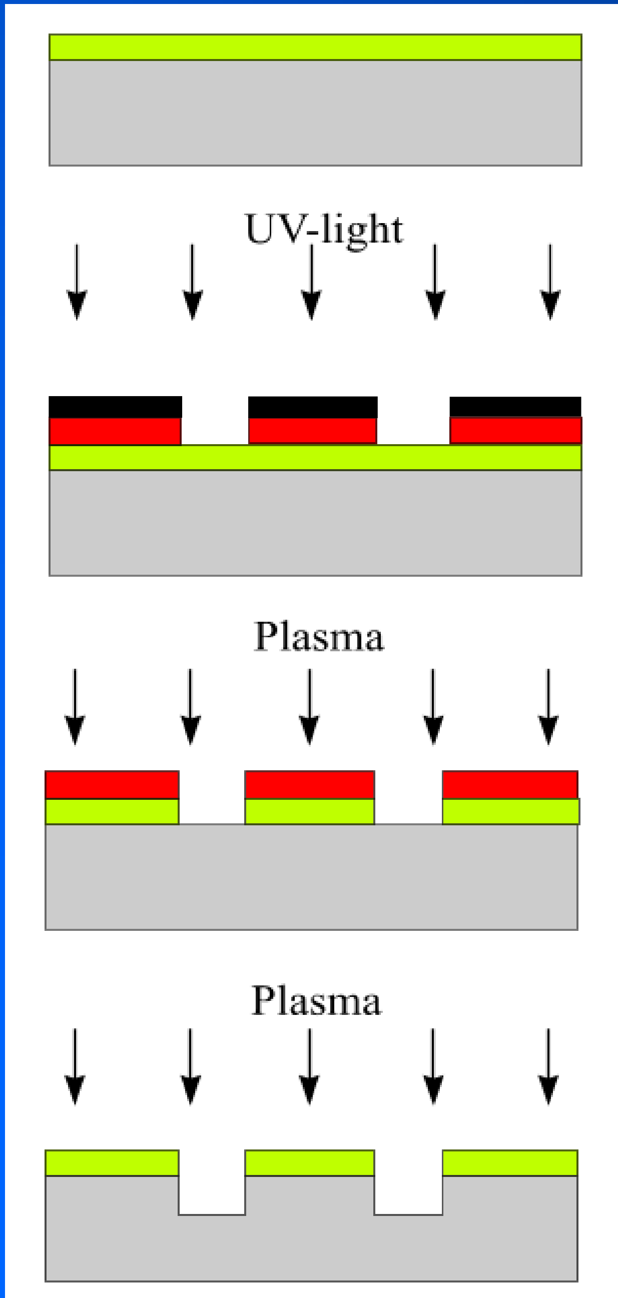

SiO_2
Si

Термическое окисление пластины Si

фотошаблон
фоторезист
SiO_2
Si

Экспонирование и проявление рисунка линз в фоторезисте

фоторезист
SiO_2
Si

Перенос рисунка линз из резиста в слой SiO_2 травлением в плазме

SiO_2
Si

Глубокое плазменное травление кремния через SiO_2

Si nanolenses

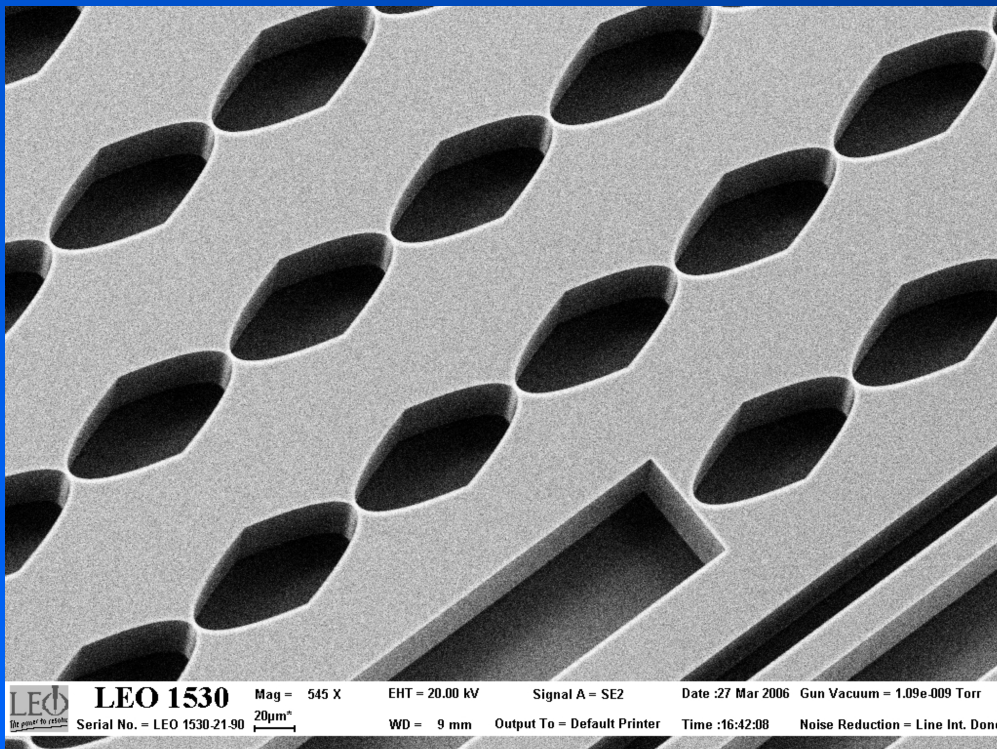

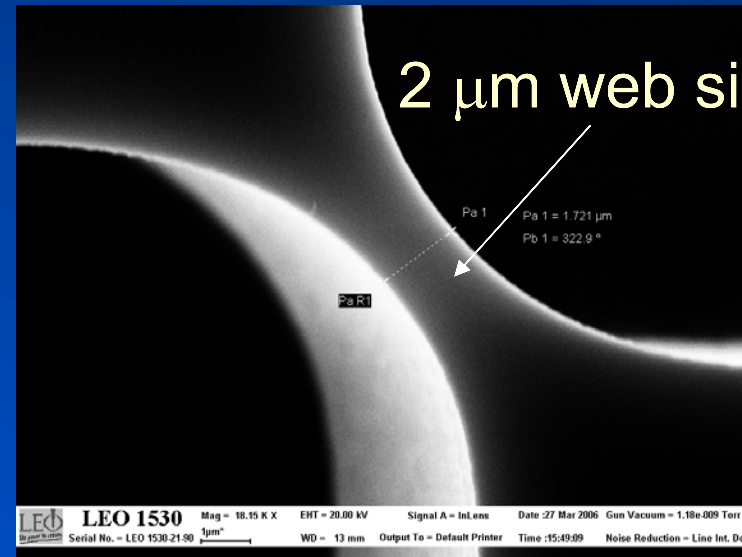

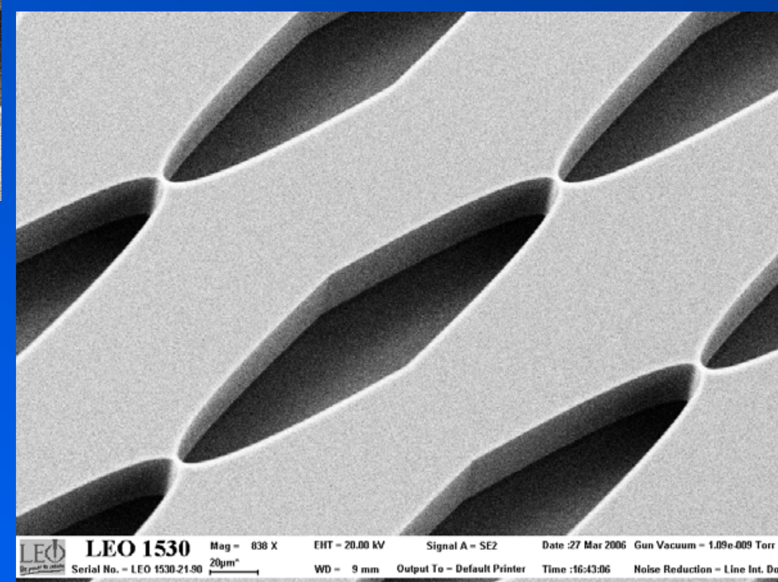

Принцип “Bosch” процесса травления кремния

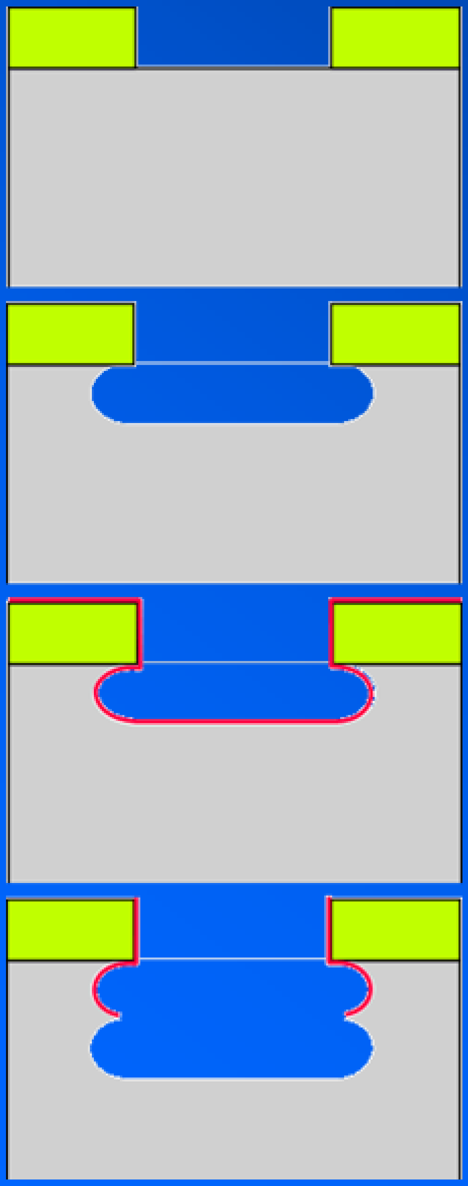

Si пластина с защитной SiO_2 маской

Изотропное травление
кремния в плазме SF_6

Осаждение полимера
в плазме C_4F_8

(новый цикл)
Изотропное травление
кремния в плазме SF_6

Уменьшение амплитуды шероховатости

Оптимизация цикла травления

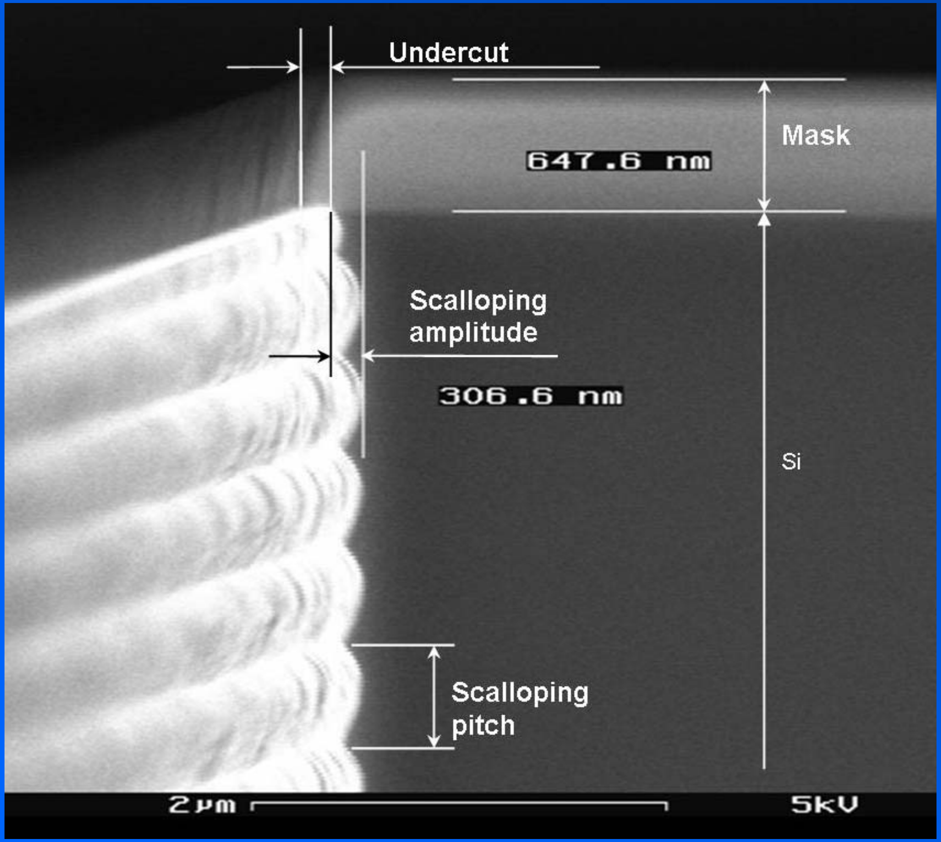

Стандартный цикл травления

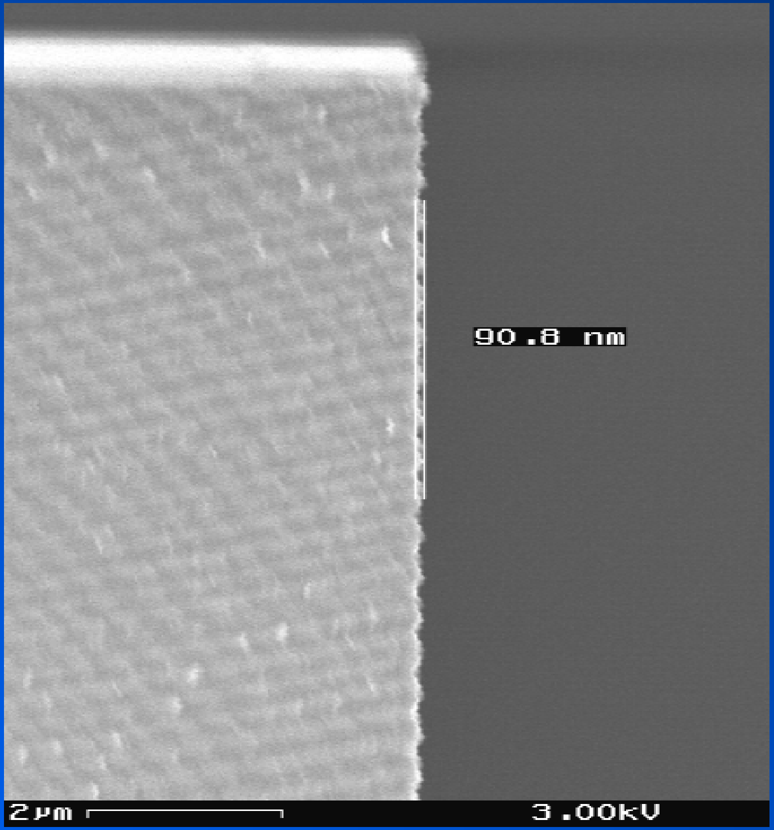

Уменьшенный цикл травления

Chip 01 Bosch process W4

Chip 07 Bosch process W5

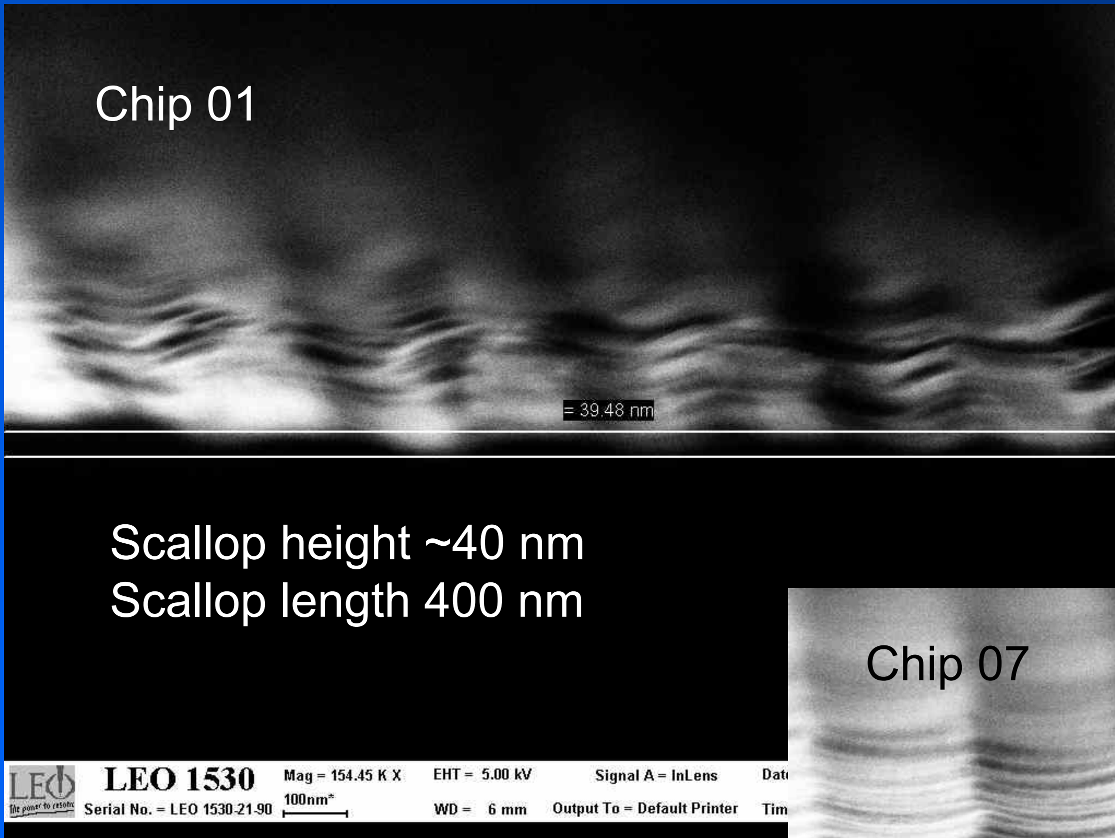

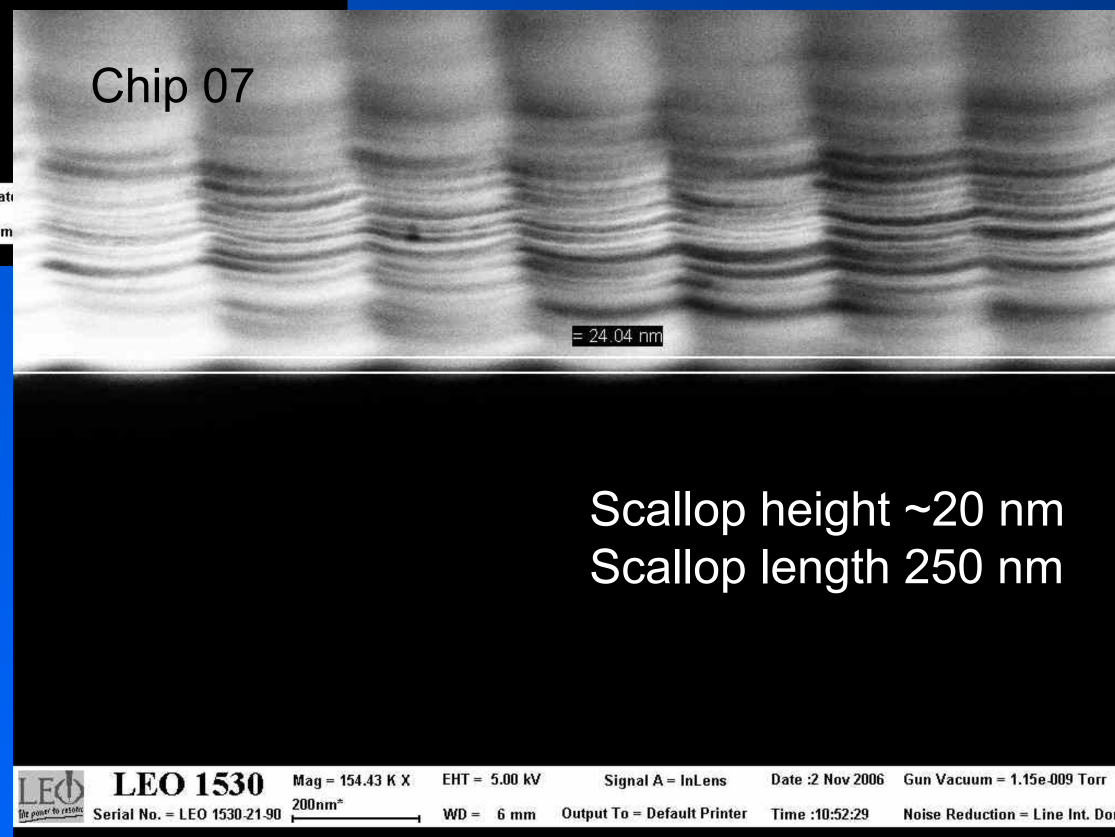

Si planar lens

ID6, Sept. 2008

F = 40 mm

E = 31 keV

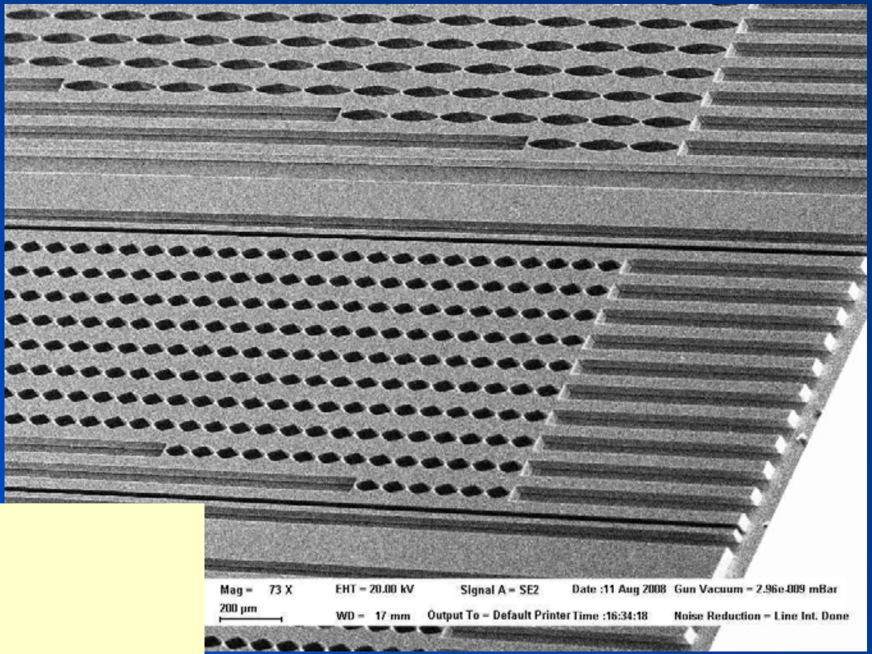

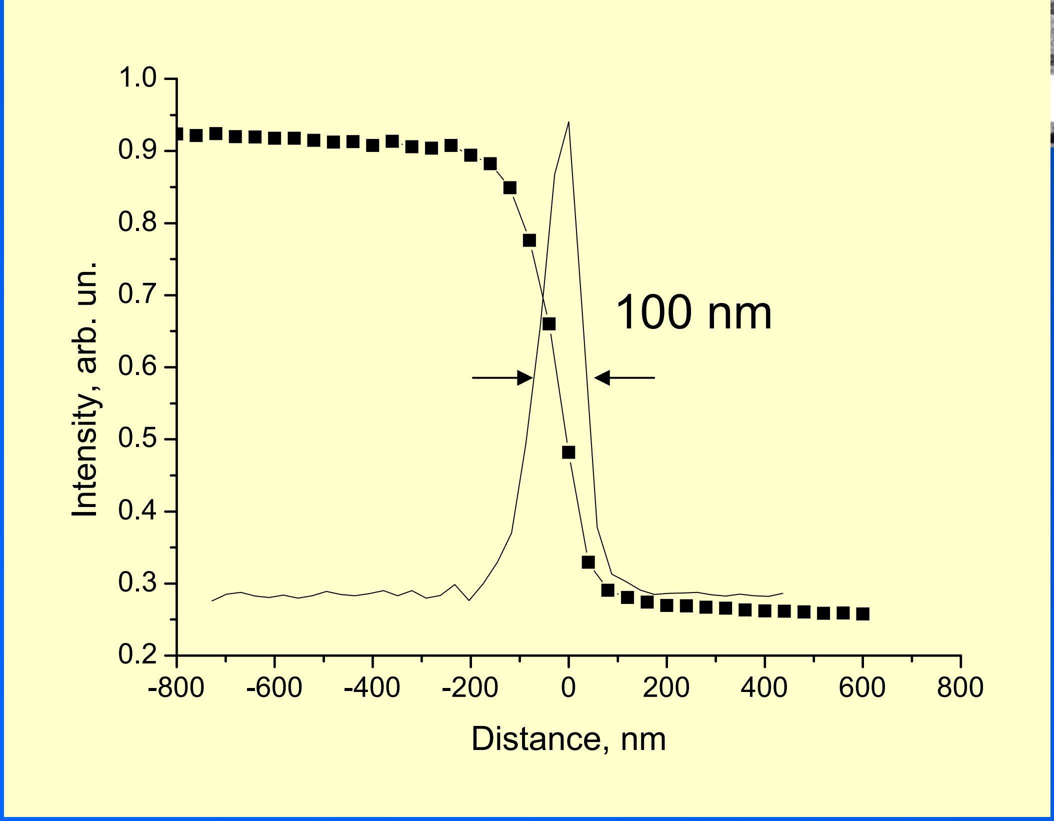

Hard X-ray Interferometers

Bonse-Hart interferometer
1965

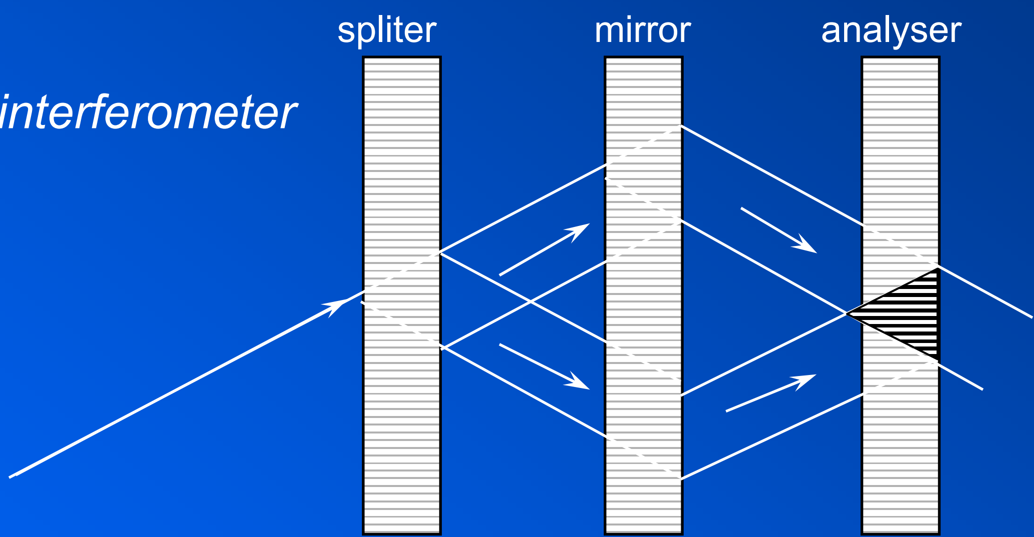

$\Lambda \sim 0.1$ nm

perfect Si crystals

X-rays

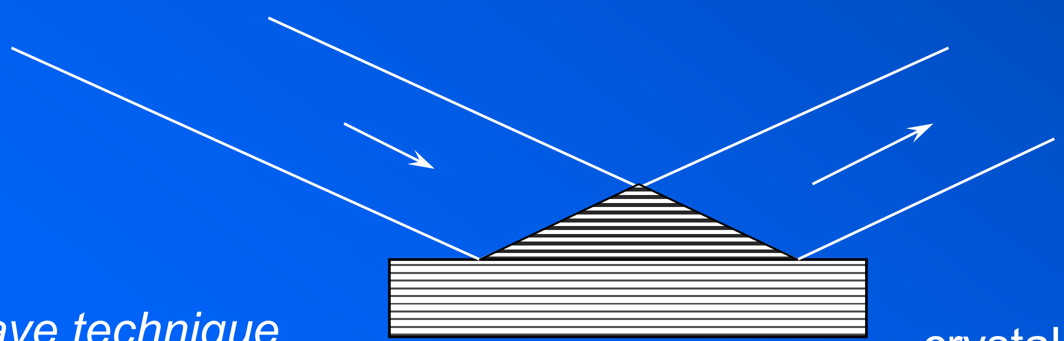

$\Lambda \sim 0.1 - 10$ nm

Standing wave technique
Battermann 1962

crystal
ML
mirror

Double slit

W. Leitenberger, S. Kuznetsov, A. Snigirev,
Interferometric measurements with
hard X-rays using a double slit
Optics Communications **191,** 91-96 (2001)

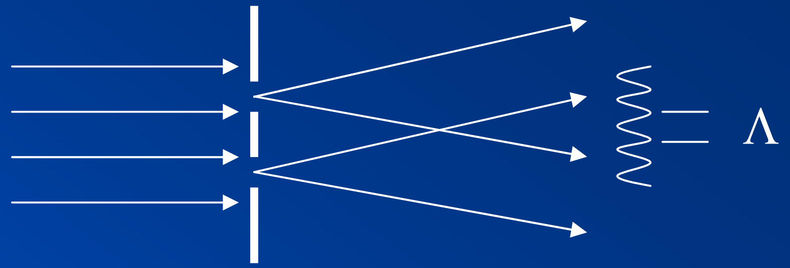

$\Lambda \sim 1$ - $10\ \mu m$

Double mirror

K. Fezzaa, F. Comin, S. Marchesini, R. Coisson, M. Belakhovsky,
X-ray interferometry at ESRF using two coherent beams from Fresnel mirrors
Journal of X-Ray Science and Technology **7,** 12-23 (1997)

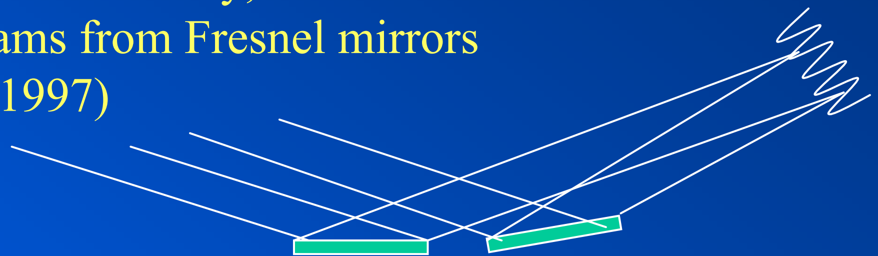

Talbot interferometer

P. Cloetens, J. P. Guigay, C. De Martino, J. Baruchel, and M. Schlenker,
Fractional Talbot imaging of phase gratings with hard x rays ,
Opt. Lett. **22**, 1059-1061 (1997)

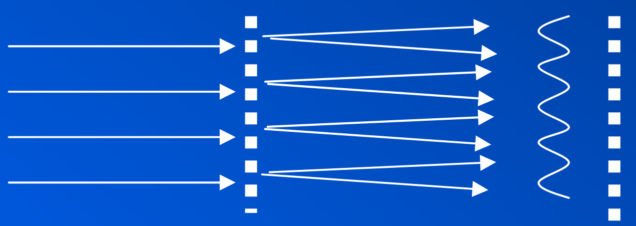

Grating interferometer

T. Weitkamp, B. Nohammer, A. Diaz, C. David, E. Ziegler,
X-ray wavefront analysis and optics characterization with a grating interferometer
Appl. Phys. Lett., 86, 054101 (2005)

Billet split lens

Professeur Felix Billet (1808 -1882)
la Faculté des sciences de Dijon depuis 1843

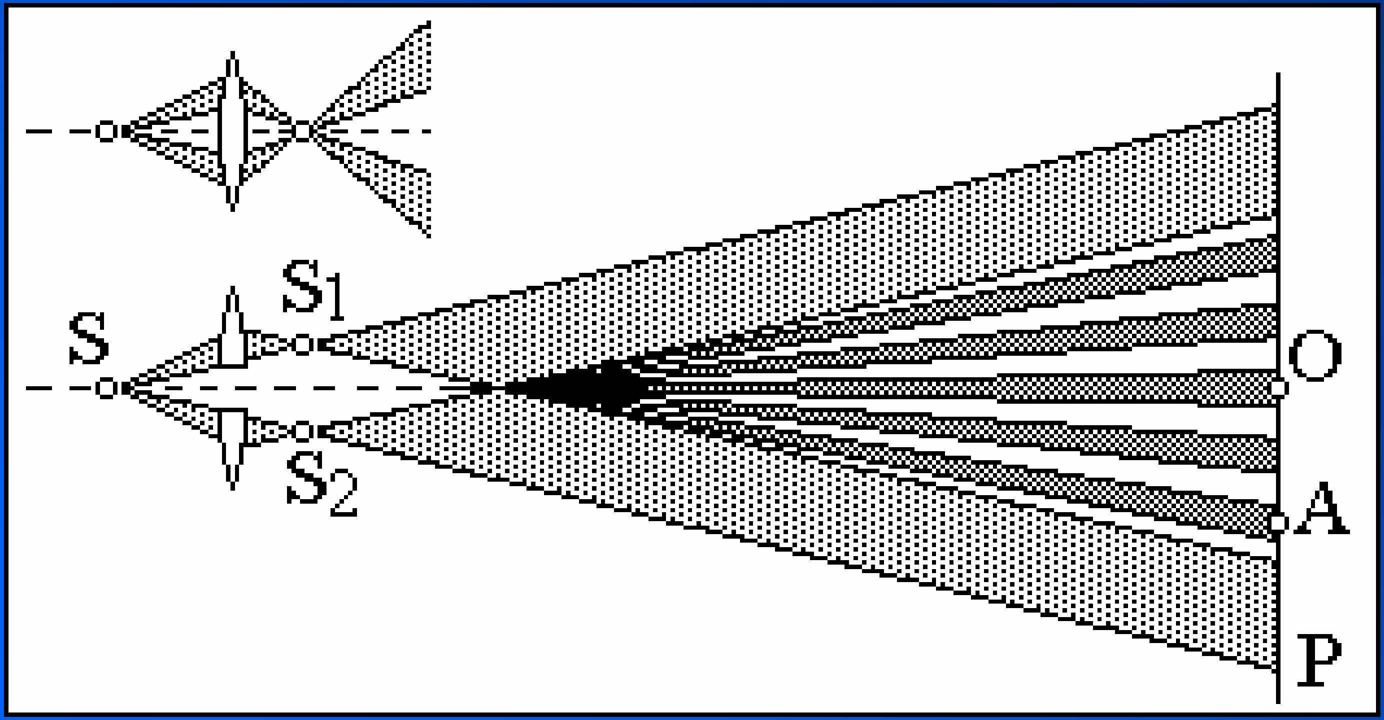

Billet split lens

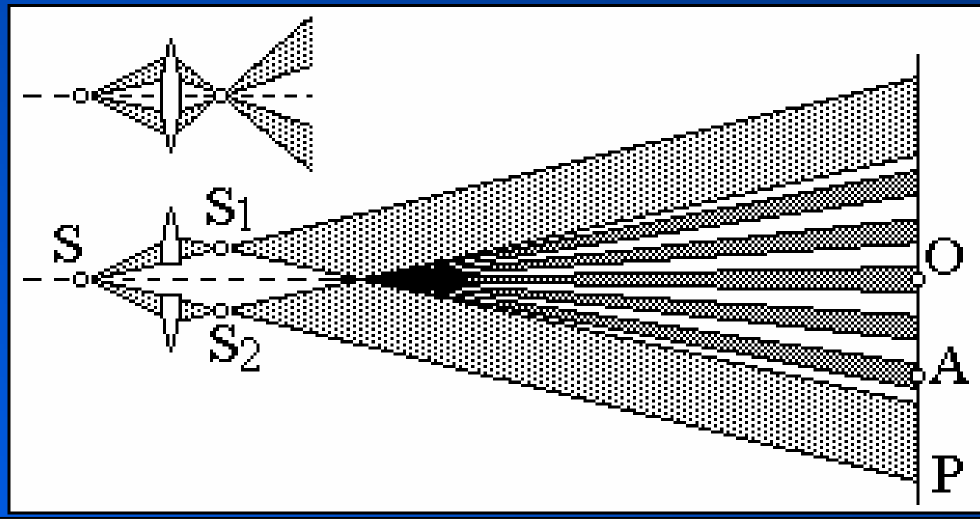

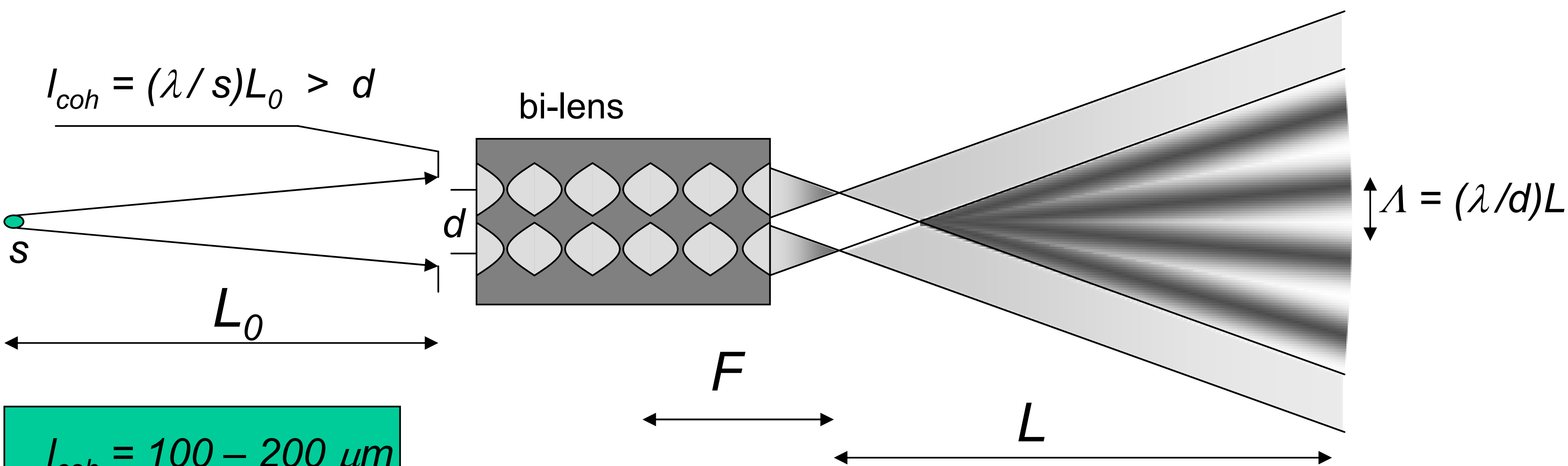

$l_{coh} = 100 – 200\ \mu m$
$E = 12\ keV$
$s = 25 - 50\ \mu m$
$L = 50m$

X-ray bi-lens

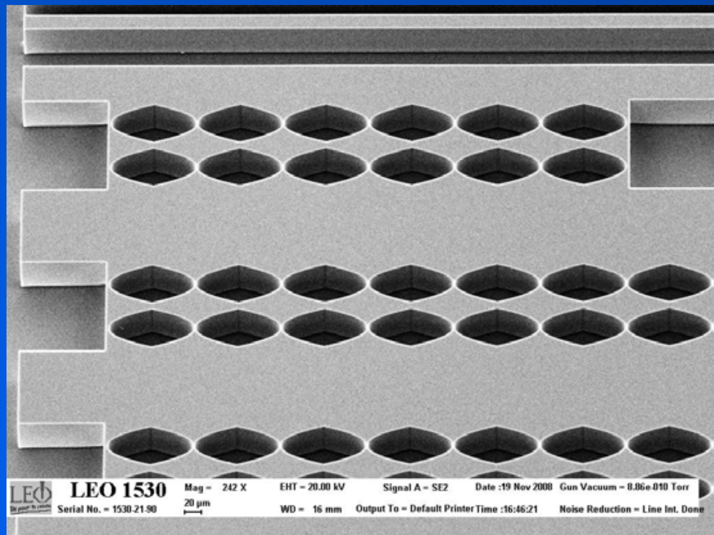

Si bi-lens chip

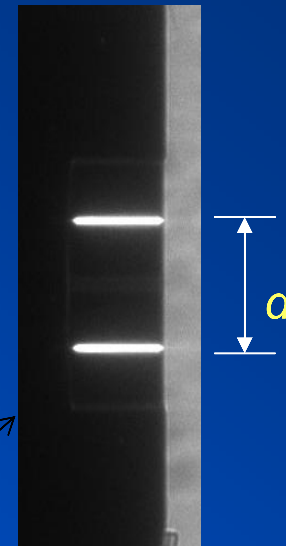

foci image

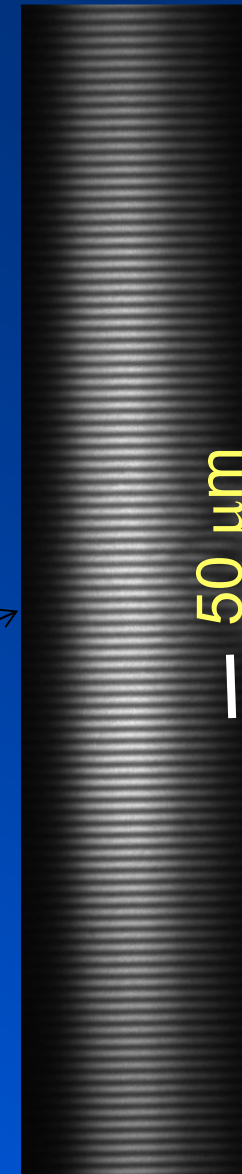

far-field interference

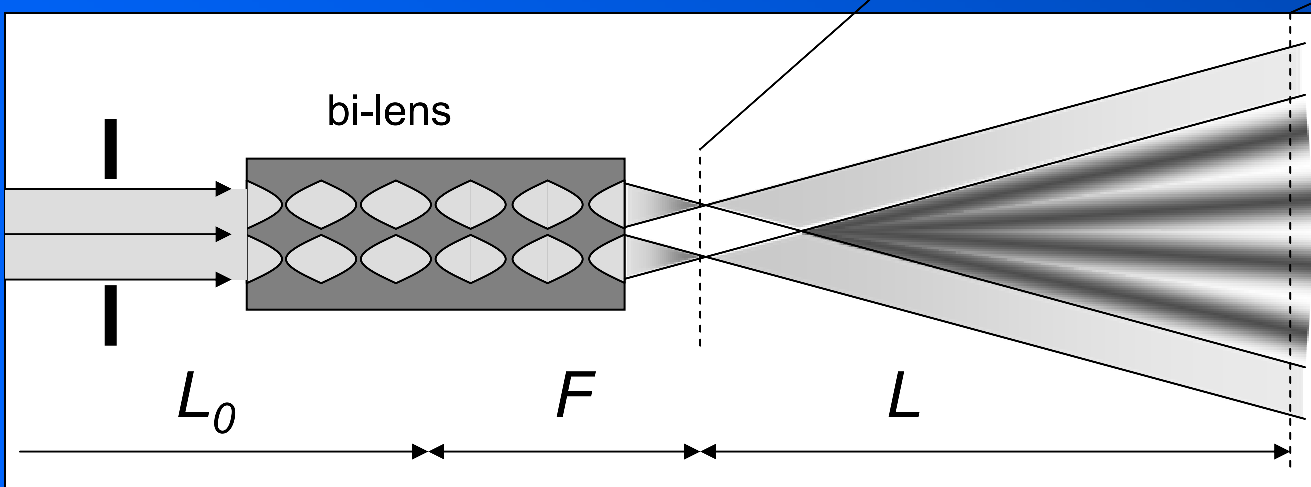

$\Lambda = \lambda L / d$

X-ray bi-lens interferometer

E = 12 keV

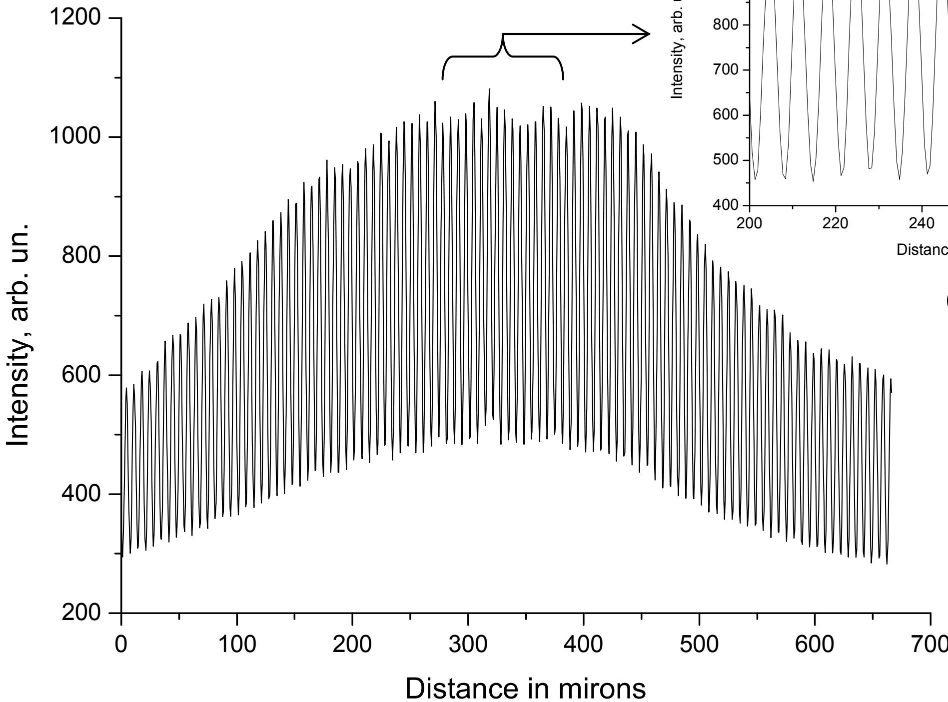

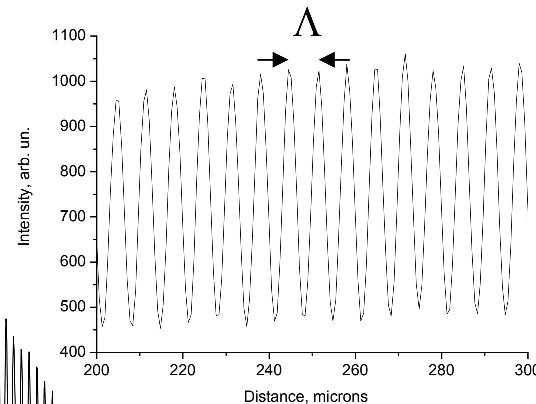

contrast C = 40%

far-field interference

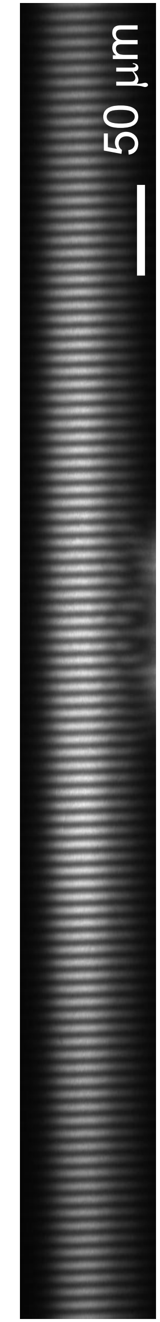

source size: $$S = \frac{\Lambda L_0}{L_1}\left(-\frac{\log C}{3.56}\right)^{1/2}$$

S = 28 μm (FWHM)

A.Snigirev, I.Snigireva, T.Roth, G.Vaughan, C.Detlefs (ESRF),V.Kohn (Kurchatov I.), M.Grigoriev, V.Yunkin, S.Kuznetsov (IMT) *ID6, October 2008*

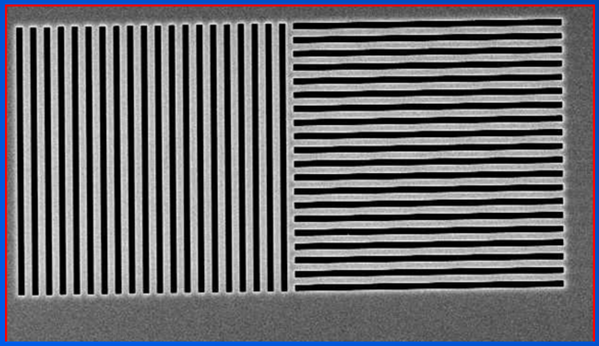

20 μm

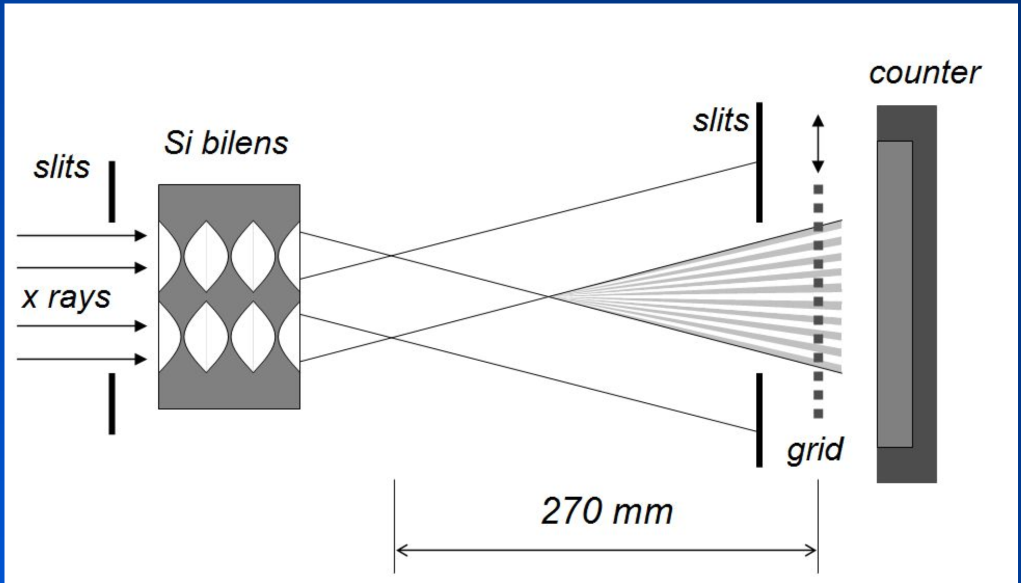
counter
slits
Si bilens
slits
x rays
grid
270 mm

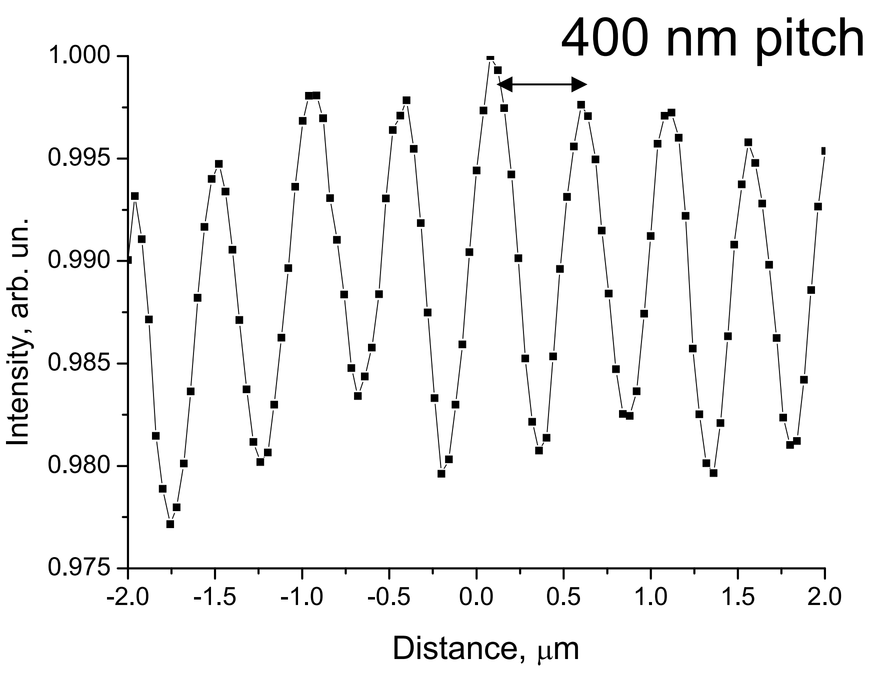
400 nm pitch
1.000
0.995
0.990
0.985
0.980
0.975
Intensity, arb. un.
-2.0
-1.5
-1.0
-0.5
0.0
0.5
1.0
1.5
2.0
Distance, μm

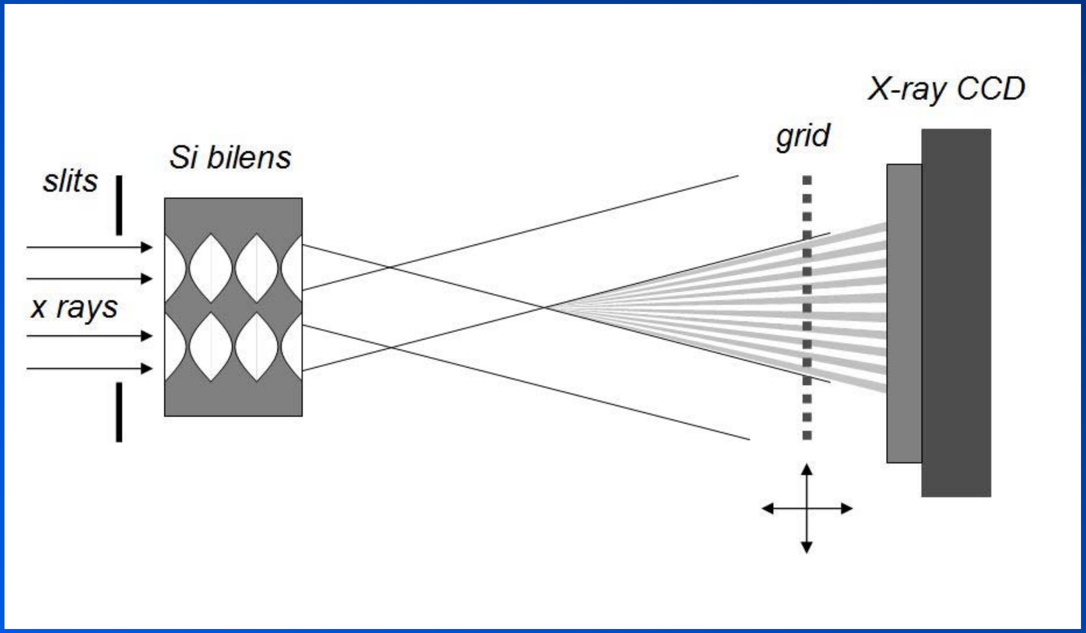

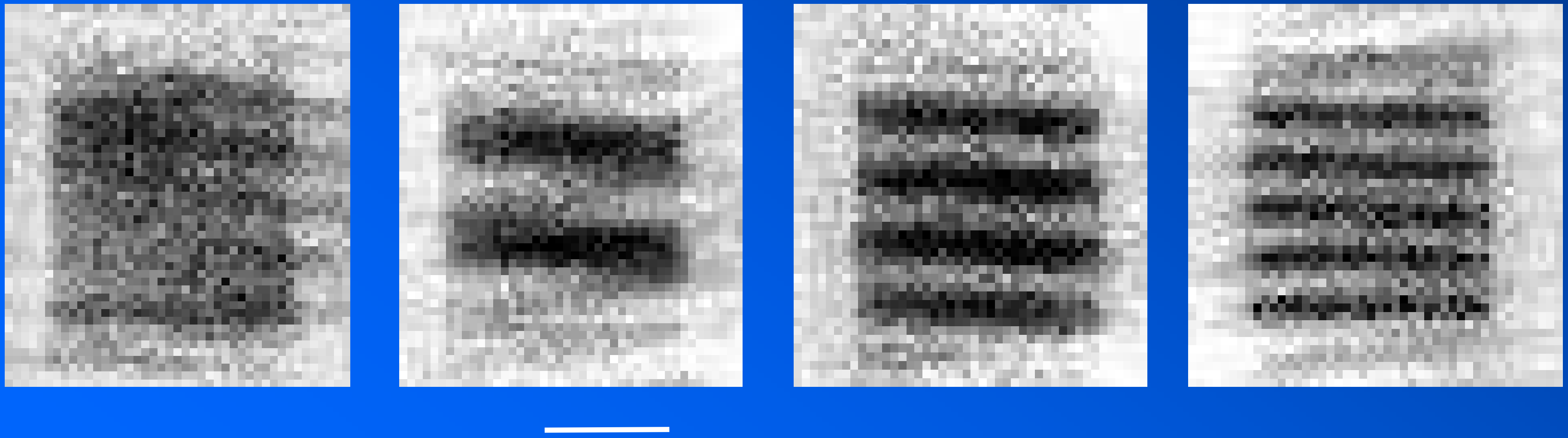

10 μm

$\Lambda_5 - \Lambda_4 = 5\ nm$!

APS » Journals » Physical Review Letters » Covers » Vol. 103, Iss. 6

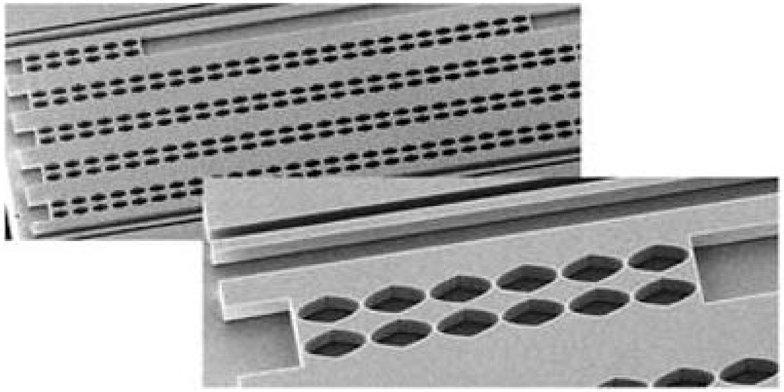

Scanning electron microscope images of silicon bilenses carefully designed to create a novel type of x-ray interferometer.

X-Ray Nanointerferometer Based on Si Refractive Bilenses

A. Snigirev,[1] I. Snigireva,[1] V. Kohn,[2] V. Yunkin,[3] S. Kuznetsov,[3] M. B. Grigoriev,[3] T. Roth,[1] G. Vaughan,[1] and C. Detlefs[1]

[1]*ESRF, B.P. 220, 38043 Grenoble, France*

[2]*Russian Research Center "Kurchatov Institute," 123182, Moscow, Russia*

[3]*IMT RAS, 142432 Chernogolovka, Moscow region, Russia*

(Received 28 April 2009; published 3 August 2009)

We report a novel type of x-ray interferometer employing a bilens system consisting of two parallel compound refractive lenses, each of which creates a diffraction limited beam under coherent illumination. By closely overlapping such coherent beams, an interference field with a fringe spacing ranging from tens of nanometers to tens of micrometers is produced. In an experiment performed with 12 keV x rays, submicron fringes were observed by scanning and moiré imaging of the test grid. The far field interference pattern was used to characterize the x-ray coherence. Our technique opens up new opportunities for studying natural and man-made nanoscale materials.

Phase contrast imaging

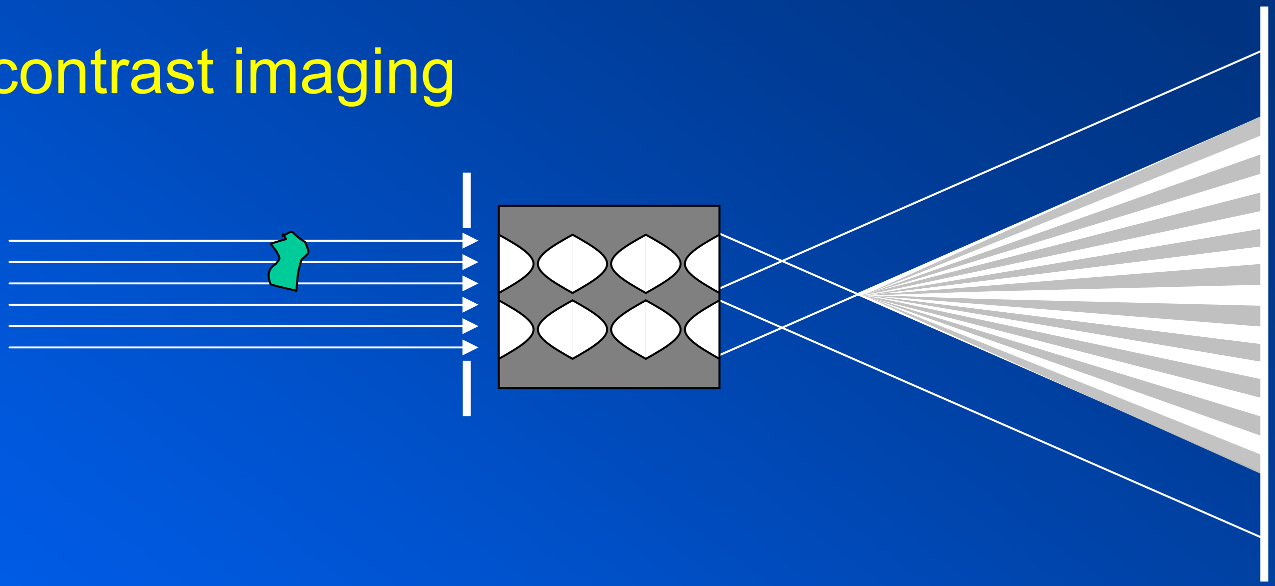

Fourier holography

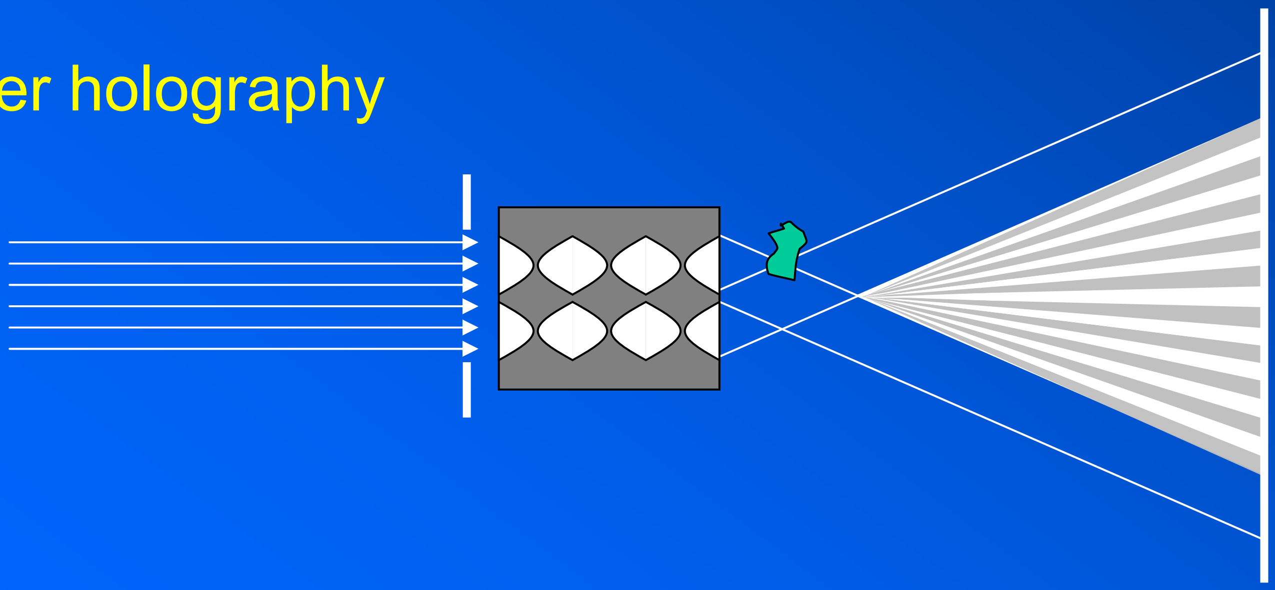

Applications

- Coherence / Optics characterization
- Interferometry – phase contrast
- Standing wave technique
- Moiré radiography
- Fourier holography
- Double slit topography

Crystal based	*0.1 – 10 nm*
Bi-lens interferometer	*10 – 1000 nm*
Grating based	*>1000 nm*

to be published in PRL, July 31 2009

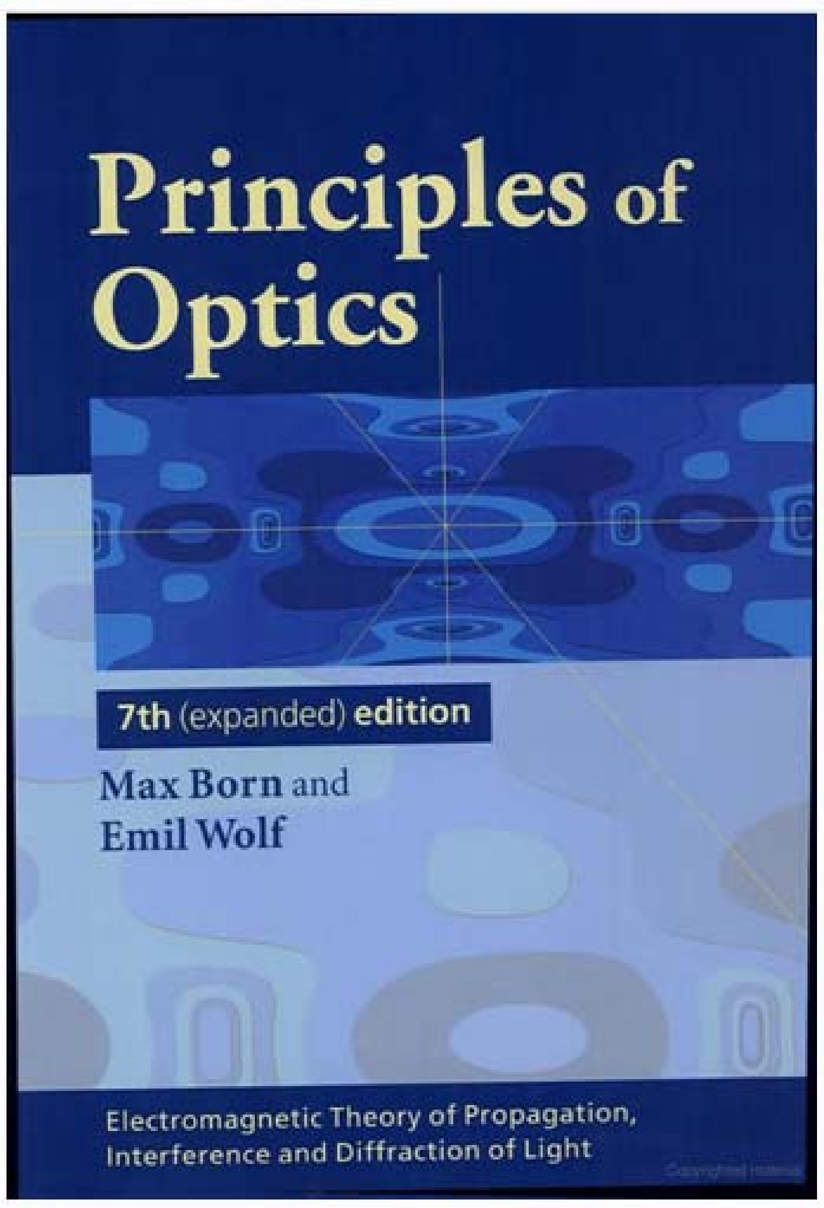

Emil Wolf

1st edition in 1959 !!

PRL **103**, 075501 (2009) PHYSICAL REVIEW LETTERS week ending 14 AUGUST 2009

Solution of the Phase Problem in the Theory of Structure Determination of Crystals from X-Ray Diffraction Experiments

Emil Wolf*

Department of Physics and Astronomy and the Institute of Optics, University of Rochester, Rochester, New York 14627, USA

(Received 6 May 2009; published 10 August 2009)

We present a solution to a long-standing basic problem encountered in the theory of structure determination of crystalline media from x-ray diffraction experiments; namely, the problem of determining phases of the diffracted beams.

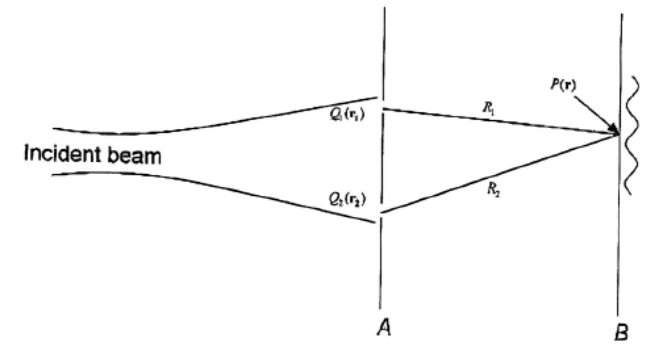

FIG. 1. Illustrating notation relating to Young's interference experiment.